J. Earth Syst. Sci. (2024)133 118
https://doi.org/10.1007/s12040-024-02311-5

Lithofacies and deformation structure of the Bandarban Anticline, Chittagong–Tripura Fold Belt, Bangladesh – Depositional environments and tectonic implications

Md Sakawat Hossain[1,*], Rumana Yeasmin[1], Md Sharif Hossain Khan[1], Md Ibna Reday[2], Fatema Tuz Zohora[3] and Samiya Tasnim Toma[1]

[1]*Department of Geological Sciences, Jahangirnagar University, Dhaka 1342, Bangladesh.*
[2]*Planning Division, Bangladesh Gas Field Company Limited, Brahmanbaria 3400, Bangladesh.*
[3]*Environment and Geology Division, Maddhapara Granite Mining Company Ltd., Dinajpur, Bangladesh.*
[*]*Corresponding author. e-mail: sakawat@juniv.edu*

MS received 23 September 2023; revised 31 December 2023; accepted 5 January 2024

The folded flank of the Bengal Basin (i.e., Chittagong–Tripura Fold Belt, CTFB) is the westward prolongation of the Indo-Burman Ranges (IBR), which developed as accretionary wedge due to the oblique subduction of the Indian Plate beneath the Burmese Plate. The tectonic evolution of this area and its control on the paleo-depositional environment has been archived in the Neogene outer IBR. Within the outer IBR (i.e., CTFB), the deformation intensity and ages of the tectonic deformation, in general, decrease from east to west. However, there is still some disagreement regarding the tectonostratigraphic evolution of this area, especially during the Pliocene and onward. The present study attempts to synthesize geomorphic, structural, lithofacies, and deformation kinematics of the area to infer the tectonostratigraphic evolution of the Bandarban Anticline and its adjacent areas. Based on geomorphic attributes and fault-related deformation structures, two sets of faults, longitudinal (NNW–SSE) and transverse (E–W), have been identified. The longitudinal faults are thrust faults running through the flanks of the structure; the fault on the western flank is the main thrust, while the fault on the eastern flank is the back thrust of the main thrust. The transverse faults are strike-slip faults that partially control the course of the antecedent Sangu River. Three major facies associations: shelf/shallow marine (FA-1; Lower Boka Bil/Upper Bhuban Formation), tide dominating delta (FA-2; Boka Bil Formation), and fluvial (FA-3; Tipam and Dupi Tila formations) have been revealed from the exposed rock formations suggest that the study area experienced different depositional settings temporally and spatially. During post-Boka Bil deposition in Pliocene–Pleistocene, the continued tectonics and/or sea level fall, the area emerged/uplifted significantly and the Tipam and the Dupi Tila formations deposited under fluvial settings. This late-stage tectonics is still going on and shaping the geomorphology of the area.

Keywords. Drainage pattern; deformation kinematics; facies association; depositional environment; tectonostratigraphy.

Published online: 08 June 2024

1. Introduction

The Chittagong–Tripura Fold Belt (CTFB), which is the folded flank of the Bengal Basin in eastern Bangladesh represents the less intensely deformed Cenozoic sediments in the foreland settings of the outer Indo-Burman Ranges (IBR) (Najman *et al.* 2012, 2022; Betka *et al.* 2018; Yang *et al.* 2020; Hossain *et al.* 2022; Khin *et al.* 2023). Exposed Tertiary sediments consist of deltaic-shallow marine to fluvial deposits with the Surma Group at the base, overlain by the Tipam Sandstone and Dupi Tila formations, respectively. The coarsening upward sequence and the sediment transport fabrics suggest basinward progradation of the deltaic sedimentation and north-easterly source terrain (Gilbert 2001; Rahman *et al.* 2020; Haque and Roy 2021). The Indian and Burmese plate's collisional history is well preserved in the CTFB sedimentary record in the form of architecture and texture of rocks, and deformation structures. The presence of numerous folded structures and other essential petroleum system elements with major faults and associated gas seepages appealed to different international oil and gas companies for drilling in the area in the 1990s (Chowdhury *et al.* 2022; Imam 2022; Shamsuddin 2022). However, due to a lack of discoveries, the folded structures of the CTFB remained poorly studied with regard to surface and subsurface geology. In this context, an attempt has been made to study the sedimentological, stratigraphic, structural, and active tectonics of the Bandarban Anticline, one of the prominent structures of the CTFB, for further hydrocarbon exploration and development activity.

The Bandarban Anticline (figure 1a) is situated within the western fold-thrust zone (WFTZ) of the CTFB (Bakhtine 1966; Hossain *et al.* 2022). The folds in the CTFB grown progressively westward and to the west of the Thrust Front (i.e., Chittagong Coastal Fault or CCF), the anticlines are broad and low relief structures (Wang *et al.* 2014; Steckler *et al.* 2016; Betka *et al.* 2018; Hossain *et al.* 2019) and therefore, their deformation intensity decreases from east to west. Accordingly, older sediments (i.e., Lower Bhuban Formation) are exposed along the axial zone of the eastern highly compressed fold-thrust zone (EFTZ) and relatively younger sediments (i.e., Upper Bhuban and Boka Bil formations) are exposed along the axial zone of the WFTZ (Hossain *et al.* 2022). The commencement of the folds in the CTFB area is assumed to have started since the Pliocene or even later as an accretionary wedge (Maurin and Rangin 2009; Najman *et al.* 2012; Khan *et al.* 2018). The structural trend and topographic relief of the Bandarban and its adjacent structures have similarities. Most of these structures are traversed by a dendritic drainage network of small streams and streamlets, controlled mostly by tectonics as well as lithology (Khan *et al.* 2017). Some of the anticlinal structures (e.g., Bandarban, Gobamura, and Sitapahar) are cut by the antecedent rivers (Valdiya 1996).

Bandarban district town, mainly located to the north of the eastern flank of the Bandarban Anticline, is one of the important hilly towns of Bangladesh with a considerable number of inhabitants and infrastructures. The town and its adjacent areas are also some of Bangladesh's most important tourist destinations due to its serenity, lush greenery, topographic beauty, and rafting opportunities in the Sangu River. Due to rapid and unplanned urbanization, the area has been subjected to major landslide hazards and has caused human casualties in the last few years, especially during heavy monsoon downpours. Limbs of the Bandarban and other high-relief anticlines of the CTFB area are locally thrusted with opposite vergent (i.e., to the east and west), some of which are possibly earthquake-inducing major thrust faults (Steckler *et al.* 2008; Wang *et al.* 2014; Hossain *et al.* 2019). As per the Bangladesh earthquake zonation map (BNBC 2020; Hossain *et al.* 2020b), Bandarban is situated in Earthquake Zone II. The presence of fault scarps, small incised streams, sharp stream bends, large-scale landslides, and quite a few earthquakes in the recent past suggest the neotectonic activity in the study area.

Several studies have been done in the CTFB and its adjacent areas to understand the geology, structure, tectonics, and geodynamics (Evans 1964; Holtrop and Keizer 1970; Johnson and Alam 1991; Reimann 1993; Gani and Alam 1999; Alam *et al.* 2003; Maurin and Rangin 2009; Najman *et al.* 2012; Dina *et al.* 2016; Steckler *et al.* 2016; Betka *et al.* 2018; Mallick *et al.* 2019; Rahman *et al.* 2020; Yang *et al.* 2020; Hossain *et al.* 2020a, 2022; Bürgi *et al.* 2021; Oryan *et al.* 2023). All these studies focus on the overall geology of the CTFB in the regional context. However, no study has been conducted on the stratigraphy, structure, tectonics, and active tectonics of the Bandarban Anticline. Therefore, in this research, the surface geology and structural data are incorporated with the subsurface geology to surmise the stratigraphy, deformation structures,

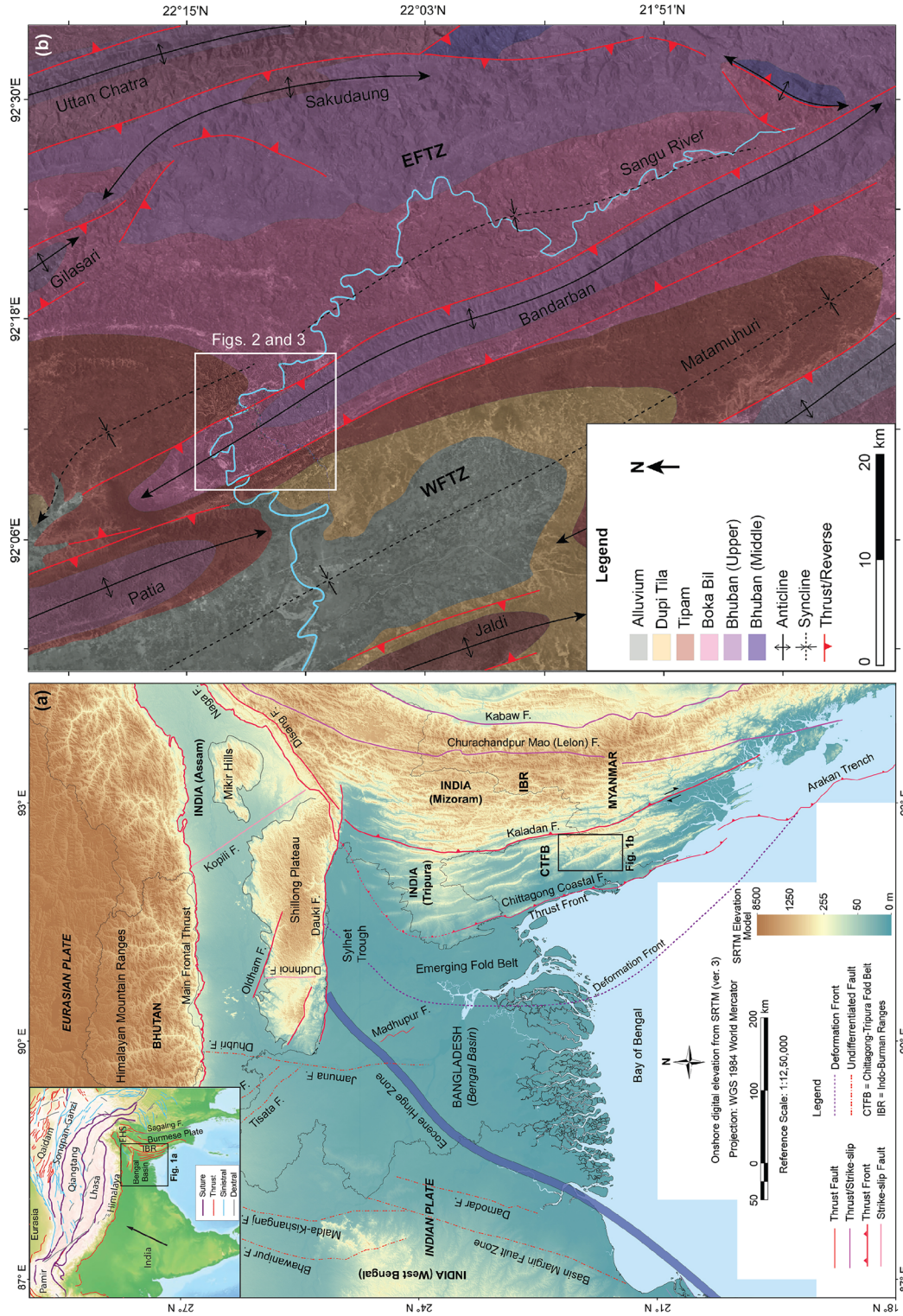

Figure 1. Tectonic map of the Bengal Basin and geological map of the CTFB area (modified after Hossain *et al.* 2022). **(a)** A generalized tectonic map of the Bengal Basin and its surroundings is superimposed on the digital elevation model (DEM) of the area. The Shuttle Radar Topography Mission (SRTM) images have been used to create the DEM. All tectonic elements are compiled from Hossain *et al.* (2019; 2020a). The CTFB area is marked with a black rectangular box. The index map (modified after Huang *et al.* 2019) shows the regional tectonic domains. **(b)** Generalized geological map of the CTFB (modified after Hossain *et al.* 2022). Note: F: Fault; CCF: Chittagong Coastal Fault; EFTZ: Eastern highly compressed fold-thrust zone; WFTZ: western fold-thrust zone. The white rectangular box is the study area (i.e., the Bandarban Anticline).

and kinematics of the area. One of the key purposes of this study is to record and interpret the exposed stratigraphy, lithofacies, deformation structures, and active tectonics based on toposheet, satellite images, geological fieldwork, sampling, and desktop analysis. The research has broad implications for enhancing the understanding of the overall stratigraphic, structural, and tectonic evolution of the CTFB area of the Bengal Basin as a whole.

2. Geomorphological and geological settings

Geographically, the Bandarban Anticline lies between the latitudes 21°18′–22°25′N and longitudes 92°10′–92°35′E (figure 1b). Physiographically, the structure is bordered on the east by the Sakudaung and Gilasari anticlines; on the north by the Sitapahar Anticline; on the west by the Patia and Matamuhuri anticlines; and on the south, the structure merges with Mowdak Anticline and then continue as single structure into Myanmar (Hossain *et al.* 2020a).

2.1 *Geomorphology*

The CTFB area has a distinct geomorphological character compared to the rest of the Bengal Basin. Brammer (2012) classified Bangladesh into 24 physiographic sub-regions. Most of the CTFB area, including the Bandarban Anticline, is named the 'northern and eastern hills' (Brammer 2014). The Bandarban Anticline is about 100 km long, ∼10 km wide, and mostly hilly terrains with Tertiary sedimentary rocks. In this structure, the hills' average elevation is ∼450 m above mean sea level (MSL), but two peaks rise to 800 m or more. The DEM suggests that the elevation of the eastern hills area is relatively higher than the western part (figure 1a). The structure has a valley only on the western side, which is linear in shape and parallel to the structural trend (figure 2). The eastern side valley is consumed by thrust faults with an en-echelon fold.

Sangu River is the major antecedent river, which mostly flows parallel to the structure with an occasional sharp bend along the eastern flank of the structure, then a bend to the west cut across the northern plunge of the structure. The study area and the CTFB as a whole are traversed by a network of small streams and streamlets. They together form a dendritic drainage network, follow the hill slopes, and are controlled by tectonic structures and lithological boundaries (Khan *et al.* 2018). Some of the major stream's courses are parallel to the main structural trend (i.e., NNW–SSE) and appear to be mainly structurally controlled. The Sawlak Khal (i.e., stream) just west of the anticlinal axis forms a longitudinal valley within the anticline, which is supposed to be developed along a fault line parallel to the fold axis.

2.2 *Geology*

The sedimentation in the eastern part of the Bengal Basin is mainly controlled by Himalayan and IBR orogeny and marine transgression-regression cycles (Alam *et al.* 2003; Rahman *et al.* 2020; Yang *et al.* 2020). Sedimentation mainly occurred in the Cenozoic time, and the basin continuously filled up through the progradation of the delta that accumulated a huge deltaic sequence (Alam 1989; Alam *et al.* 2003; Rahman *et al.* 2020; Yang *et al.* 2020). The tectonic development of the eastern folded flank of the Bengal Basin, i.e., the CTFB, is due to the shortening and thickening of the upper part of the huge deltaic sequence caused by the still-ongoing collision between the Indian and Burmese plates (Steckler *et al.* 2008; Wang *et al.* 2014; Khan *et al.* 2017; Yang *et al.* 2020; Rahman *et al.* 2020; Hossain *et al.* 2022).

2.2.1 *Tectonic setting*

The Chittagong–Tripura Fold Belt (CTFB) extending from the juncture of the Naga, Disang, Dauki, and Halflong thrusts to the north and up to the Arakan Trench in the south has been recognized as the outer edge of the Indo-Burman Ranges (IBR). This western Neogene outer edge of the IBR is separated from the eastern Palaeogene IBR along the Kaladan Fault (Maurin and Rangin 2009; Gahalaut *et al.* 2013; Wang *et al.* 2014; Betka *et al.* 2018; Yang *et al.* 2020). Geologically, the central foredeep basinal part of the Bengal Basin is situated on the western side, whereas the Palaeogene IBR is situated on the eastern side of the CTFB and it is considered to be a young and active orogenic belt (figure 1). Structurally, the CTFB is separated from the central foredeep of the Bengal Basin to the west and IBR to the east by two approximately N–S running major faults. The eastern boundary of the CTFB is marked by the Kaladan Fault, which is also known as the Tut

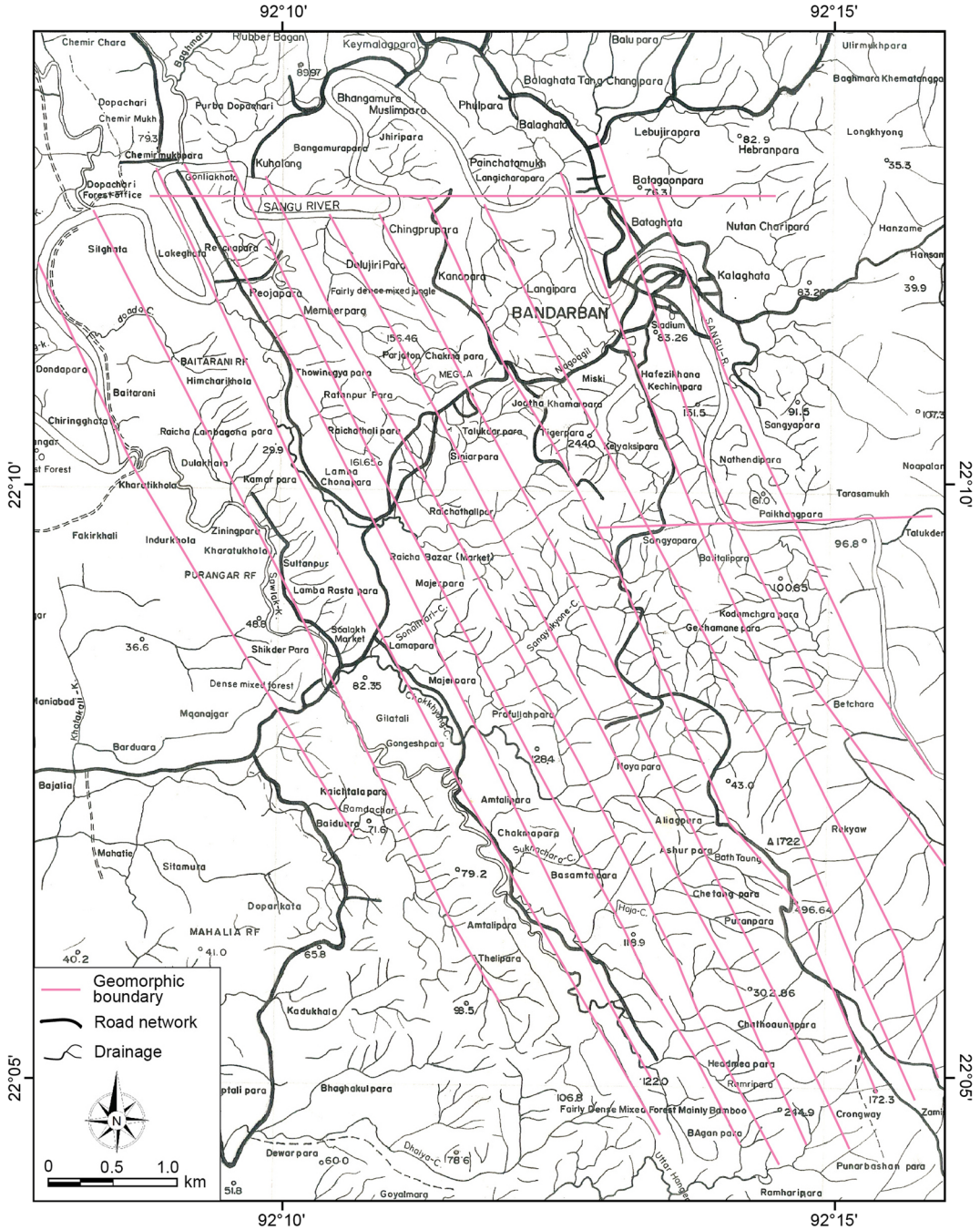

Figure 2. Base observed geomorphic features – linear features identified on the drainage map based on streamlet/river morphology/characteristics.

Fault, and the western boundary is transitional and marked by the convex shape 'Thrust Front' represented by the Chittagong Coastal Fault (CCF) (Betka *et al.* 2018; Hossain *et al.* 2020a, 2022). Although the eastern Bay of Bengal's coast parallel CCF and Kaladan River parallel Kaladan Fault are considered mostly as regional thrust faults (Betka *et al.* 2018; Vorobieva *et al.* 2021; Hossain *et al.* 2022), Maurin and Rangin (2009) considered that both the CCF and the Kaladan has dextral-slip component. The CTFB is tectonically deformed as a fold-thrust zone (i.e., mainly as echelon plunging folds and thrust faults) (Davis 1996; Hossain *et al.* 2022). To the west of the CTFB (i.e., into the current foredeep basin), Indo-Burmese subduction-related deformation continues, but the deformation intensity progressively decreases from the thrust front towards the

west and ceases along the deformation front (Betka *et al.* 2018; Hossain *et al.* 2022; Oryan *et al.* 2023). A young and gentle fold belt of ∼80 km in width slowly but continuously develops in the subsurface between the thrust front and deformation front, known as the emerging fold belt (Hossain *et al.* 2020a).

At the initial stage of the India–Eurasia and the Indian–Burmese plates convergence, the present day CTFB area was part of the Bengal Foredeep (Alam *et al.* 2003). The commencement of the CTFB as a separate structural entity in the eastern part of the Bengal Foredeep Basin as an accretionary wedge of the IBR is related to the oblique subduction of the Indian Plate beneath the Burmese Plate since the Pliocene (Steckler *et al.* 2008; Maurin and Rangin 2009; Najman *et al.* 2012; Yang *et al.* 2020; Oryan *et al.* 2023). As the subduction continues, the eastern part of the Bengal Foredeep Basin tectonically evolved as a frontal accretionary wedge, known as the CTFB or the folded flank part of the Bengal Basin. In the last 2 Ma, the tectonically uplift of the Shillong Plateau and the resulting subsidence and sedimentary filling of the Sylhet Trough facilitated the rapid westward propagation and structural development of the CTFB (Maurin and Rangin 2009; Hossain *et al.* 2021). Consequently, the intensity and the age of tectonic deformation gradually decrease westward from the IBR to the CTFB. The CTFB area has been divided into two broad tectonic domains: (i) western fold-thrust zone (WFTZ) and (ii) eastern highly compressed fold-thrust zone (EFTZ) (Hossain *et al.* 2020a).

The subduction-related tectonics are deforming the upper deltaic sediments of Tertiary Age (table 1) that occur above a major basal detachment at a depth of ∼5–7 km in the CTFB area (Sikder and Alam 2003; Steckler *et al.* 2008; Maurin and Rangin 2009; Bürgi *et al.* 2021). In the last

Table 1. *Stratigraphic succession of the Bandarban Anticline, Chittagong–Tripura Fold Belt (modified after Alam and Quaraishi 1985; Hossain et al. 2019, 2022)*

Age (approx.)		Group	Formation	Lithology	Thickness max. (m)	Depositional environment	Tectonic events
Holocene			Alluvium	Channel deposits comprise sand, silt, pebbles and boulders	–	Fluvial	Folding in the eastern Bengal Basin and initiation of the Chittagong Coastal Fault (CCF)
Plio-Pleistocene			Dupi Tila	Fine to very fine ferruginous sandstone interbedded with thick mudstone; numerous mud clasts and quartz pebbles in sandstone	∼600	Fluvial	
		Tipam	Tipam	Medium to fine-grained yellowish-brown sandstone, cross-bedded, ferruginous, contains fossil wood, minor intercalation of mudstone	∼1,600	Fluvial	Dauki Fault
Miocene	Late Miocene	Surma	Boka Bil	Dark grey shale, sandy shale and sandstone; flaser-, wavy- and lenticular-bedding dominant; numerous calcareous fine sandstones to siltstone bands are present	∼1,400	Tidal-deltaic	Shelf-slope setup, and initiation of the Kaladan Fault at the eastern edge of CTFB at the Late Miocene
	Middle Miocene		Bhuban	Bluish gray shale; sandstone and bands of calcareous siltstone present in upper part; grayish sandstone interbedded with shale and mudstone in lower part	2,500+	Shallow marine	

2 Ma, these sediments above the master basal detachment deformed through a combination of thick-skinned and thin-skinned tectonic processes and resulted in a series of ∼NNW–SSE trending curvilinear en-echelon plunging folds mainly to the east (Maurin and Rangin 2009; Betka *et al.* 2018; Hossain *et al.* 2019; Shahriar *et al.* 2020). In most cases, longitudinal fold axis parallel thrust cuts both the limbs of these anticlines (figure 1). The geometry of the CTFB fold is attributed to tens to more than 100 km long fold ridge along the strike, the free westward migration of fold, longitudinal west verging master thrust accompanied by east verging back thrust (Khan *et al.* 2017; Hossain *et al.* 2022). In some places, active macro gas seepages were encountered during fieldwork in the CTFB area, and these were also reported in earlier studies. The presence of such seepages suggests the potential presence of hydrocarbon in this area (Boruah *et al.* 2022).

The present study area (figure 1b), i.e., the Bandarban Anticline, mainly falls within the western fold-thrust zone; the southernmost part of this structure falls into the eastern highly compressed fold-thrust zone. It is one of the largest and structurally complex anticlines of the CTFB area, which was previously unexplored in detail and is supposed to provide further evidence for a proper understanding of the Tertiary sediments and deformation structures and will enable the interpretation of the petroleum system in the CTFB area.

2.2.2 *Stratigraphy*

The sedimentary sequence of the Chittagong–Tripura Fold Belt (CTFB) consists of a wide variety of siliciclastic sedimentary rocks from sandstone to shale. The total thickness of the exposed sediments in the Bandarban Anticline is about 6000 m, which provides no difference in overall lithology compared to the lithology of other anticlines at the Chittagong–Tripura Fold Belt (Alam and Quaraishi 1985; Khan 1991; Reimann 1993). The rock sequences of the Upper Bhuban, Bokabil, Tipam, and Dupi Tila formations are exposed in this anticline (table 1). This stratigraphic succession is of Neogene in age and is thought to deposit major deltaic to fluvial systems due to repetitive transgressive and regressive phases that resulted from tectonic activities and relative sea-level changes (Alam *et al.* 2003).

3. Methods

The study approach involves the synthesis of the geomorphology, surface geology, lithofacies, and deformation kinematics with the regional tectonics and stratigraphy to determine the overall structural and tectonostratigraphic evolution of the Bandarban Anticline. Geomorphology can be an excellent tool for exploring the geology of an area (Khan *et al.* 2018). Geomorphological observations from the base map and their ground checking through the field reconnaissance provide first-hand knowledge of the structure and tectonics of an area. Among the surface morphological attributes, drainage morphology is mainly used in this study, which includes (i) drainage initiation and confluence or convergent drainage, (ii) drainage bend or offset, (iii) course of the drainage, (iv) scarp and break in slope in the satellite images, and (v) the presence of linear valley. These drainage morphological features are considered to infer the lithological or structurally controlled linear features prior to fieldwork. During the field investigation, the attitude of the bedding and structural features and the lithological features of the exposed sedimentary sequences were recorded in detail, together with their geo-referenced dataset. Both structural (e.g., axial zone, fault) and lithological boundary (e.g., unit or formation boundary) datasets are then correlated with the drainage morphological features, especially the knick points from the drainage map. A drainage map of the study area has been prepared based on the available 1:50,000 toposheets obtained from the Survey of Bangladesh in conjunction with the Landsat 7 and 8 images obtained from the USGS (figure 2).

In the study area, surface outcrops are sparse due to dense vegetation cover, rapid erosion of the soft sediments, and ever-increasing settlement. During the field investigation, data were collected only from the road cut, the Sangu River cut, and some major drainage cuts that traverse across the structure. Lithological boundary and fault plane identified along different transects were manually extended across the transect with the help of a hillshade image created from a DEM using the 30 m resolution SRTM images. Secondary datasets related to the structure and tectonics of the neighbouring regions were collected from the published maps and then compared with this study's primary field dataset to see the present datasets' consistency. Based on the bedding attitude, surface lithology, exposed deformation structures (e.g.,

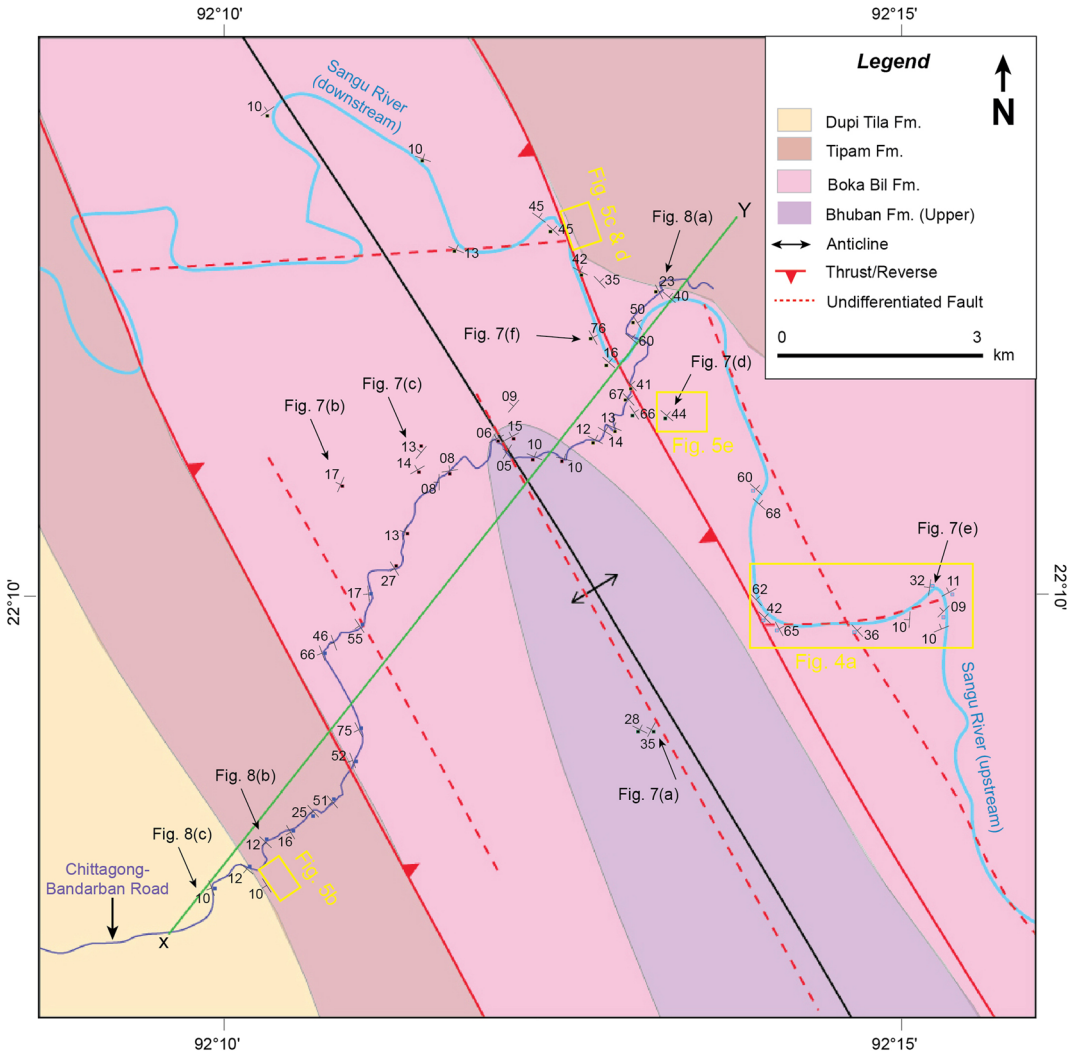

Figure 3. Surface geology map of the northern part of the Bandarban Anticline mainly along the Chittagong–Bandarban Road cut section and the Sangu River section. The main datasets are primary field data, interpretation of the drainage map (figure 2), and secondary published data (Rahman *et al.* 2020; Hossain *et al.* 2022). Note: Faults are marked with red lines, the fold axis is marked with black line, and study locations are plotted as rectangles.

fault, joint), and drainage morphology, a geologic map of the Bandarban Anticline has been prepared (figure 3).

3.1 *Bedding and deformation kinematic analysis*

To quantify the geometry of the Bandarban Anticline, the bedding attitude data (total $n = 51$) were collected along different transects and from both flanks of the structure (figure 4). The poles to the bedding planes were plotted and analyzed on Schmidt's equal area lower hemisphere projection (Lisle and Leyshon 2004; Rowland *et al.* 2007) using the software Stereonet v.11 (Cardozo and Allmendinger 2013). The density contour diagram of the bedding pole was constructed with Kamb contour (Kamb 1959). The structural orientation was determined using a cylindrical best fit of the bedding plane poles (Hossain *et al.* 2022). The bedding to mean pole orientation was determined following the right hand rule (RHR), pi-axis orientation, and the interlimb angle of the structure was determined using the same software (Allmendinger *et al.* 2012; Cardozo and Allmendinger 2013). Rose diagram based on the bedding strike orientation was constructed with a 5° class interval. To perform the kinematic analysis of the mesoscale deformation structures, bedding and fault slip attitude data (e.g., rake, displacement), as well as their mutual relationship with respective anticlinal structures, were measured, and oriented field photographs, were taken and recorded during field geological investigations. These datasets are then processed and analyzed in the laboratory

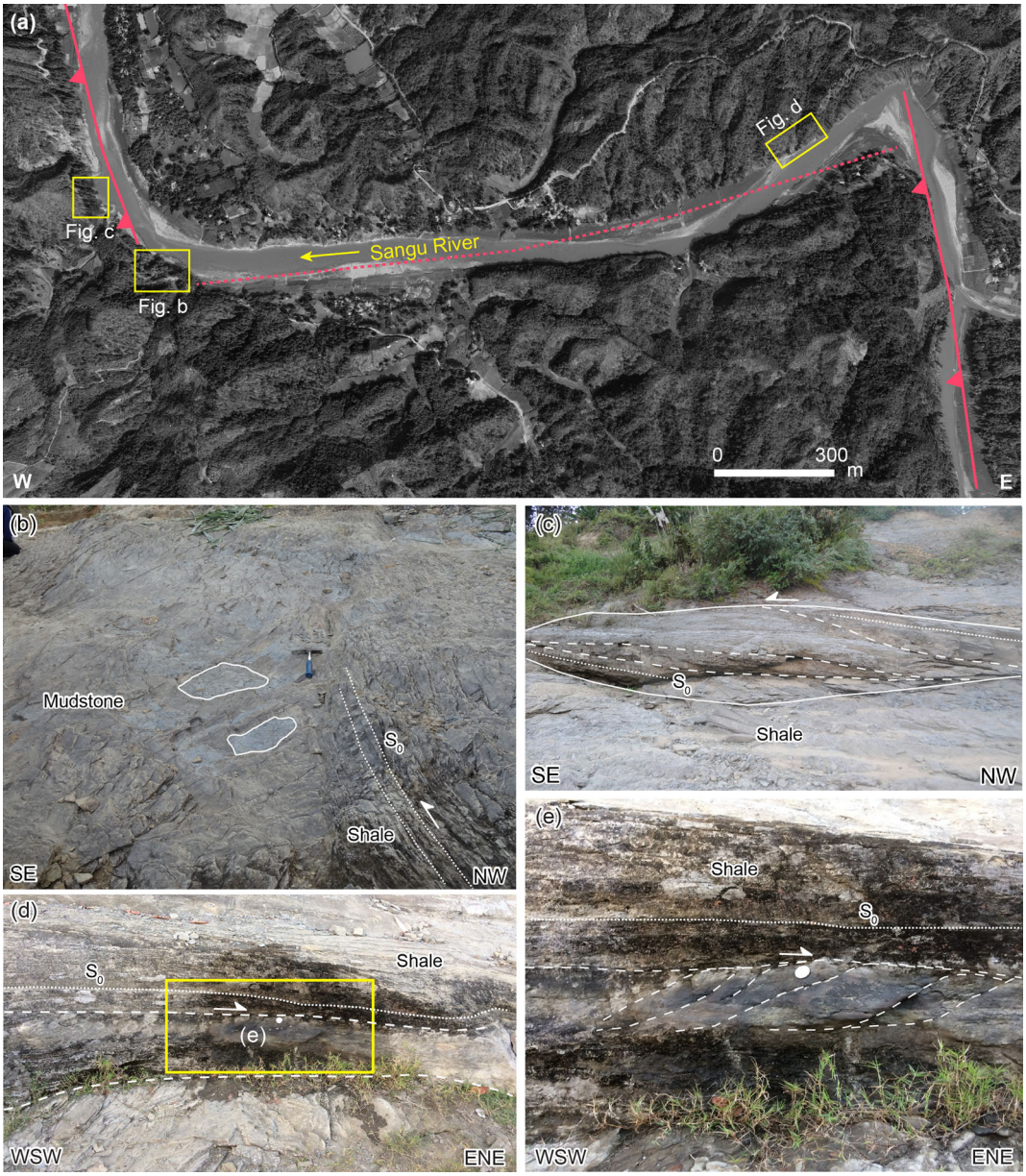

Figure 4. **(a)** The Google Earth Pro panchromatic satellite image showing the upstream Sangu River section. The location of this image is marked in figure 3. Faults are marked with red lines. The yellow rectangles represent the locations of figures (b–d). **(b)** Near vertical and highly compressed bed shows evidence of both thrust as well as shear movement. The possible sigmoidal structure is marked by white outlines formed through intense deformation of the shale bed, indicating the shear movement. **(c)** The well-developed sigmoidal structure indicates the top to the left (approximately eastward) shear movement. The length of this structure is ∼11 m. **(d)** Near the horizontal end segment of the east verging thrust. The white broken line marked the thrust plane. The diameter of the coin in the picture is 2.5 cm. **(e)** Contractional duplex structure at the near horizontal part of the east verging thrust. The duplexes are marked with white broken lines. The diameter of the coin in the picture is 2.5 cm. The location of the figure is marked with a rectangle in figure (d). In all cases, a half-arrow indicates the direction of movement.

using appropriate software (e.g., Adobe Photoshop CS6, Adobe Illustrator CS6).

3.2 *Geological cross-section*

A 2D structural model or geological cross-section was prepared based on the field datasets and previously published section of the adjacent region to comprehend the shortening of the Tertiary sediments and structural pattern of the Bandarban Anticline (Maurin and Rangin 2009; Najman *et al.* 2012; Khan *et al.* 2018; Burgi *et al.* 2021; Hossain *et al.* 2022). For the geological cross-section, profile lines are chosen across to the general trend of the bedding and fault planes, which are parallel to the NNW–SSE-directed structural trend. Hence, the

formation layers and the fault planes in the cross-section are predominantly oriented perpendicular to the maximum direction of shortening (Hossain *et al.* 2022). Dips of each layer and fault planes projected along with strikes on the cross-section. The existence of basal detachment and the continuity of the subsurface structure was postulated based on the available nearby seismic sections (Burgi *et al.* 2021), and the kink method was used to project the surface data downward (Dahlstorm 1969; Woodward *et al.* 1989). For the cross-section construction, it is assumed that there was no volume loss during the deformation after the deposition of the Tipam Formation.

3.3 *Sedimentological logging*

The Neogene successions of the Bandarban Anticline were measured and logged in detail in three sections: the Chittagong–Bandarban Road cut section, the Sangu River section, and the Shaila Propat section (figures 8 and 9). The sedimentary sequence is discontinuously exposed in all of these sections. Only the Chittagong–Bandarban Road cut section encompasses all four formations, from the oldest upper Bhuban to the youngest Dupi Tila Formation. In each section, the lithofacies were described and interpreted in terms of lithology, texture, sedimentary structures, and possible cementing materials. The facies associations were established based on the tempo-spatial relationship and similarity of the lithofacies described with regard to diagnostic sedimentary characteristics.

4. Result

4.1 *Stream morphology*

Eight linear features have been identified on the drainage network map (figure 2) prior to fieldwork, mainly based on the criteria of stream straightness, stream offsetting/bend, stream initiation, confluence, and scarps and breaks in slope criteria. It is presumed that the lines drawn on the drainage maps possibly reflect some surface and subsurface geological attributes of special interest, such as fault, lithologic boundary, fold axis, etc. During the field investigation, local surface geological features have been compared and cross-checked with the position and trend of the linear features. It is observed that the general trend of these linear features is NNW–SSE and is mostly parallel to each other. In general, most of the linear features show greater longitudinal continuity and few of them extend from one end to the other end of the structure. In addition to the drainage network, the antecedent Sangu River in the eastern and northern parts of the structure shows at least ten sharp bends within the study area.

4.2 *Surface geology*

A surface geological map (figure 3) of the Bandarban Anticline has been prepared along the Chittagong–Bandarban Road cut section and the Sangu River section mainly based on the geological fieldwork, satellite imageries, toposheets, and previously published maps (Alam *et al.* 1990; Davis 1996; Khan *et al.* 2018; Rahman *et al.* 2020; Hossain *et al.* 2022). Structural features such as fold axis and faults, and lithological boundaries have been identified and extended up to limited distances on both sides of the road cut and river sections. Other deformation structures, such as joints, cleavage, shear bands, etc., are also identified and correlated with the major structures (i.e., fault and fold) to understand the deformation kinematics. Based on the lithological characters, four rock units have been identified along the Chittagong–Bandarban Road cut section and three rock units have been identified along the Sangu River section (table 1, and figure 3).

Two major faults have been identified in the study area, which is mostly persistent, with thickness varying from m to several tens of m, and approximate lengths of more than 10 km. One fault (060°/35°) was identified along the Chittagong–Bandarban Road cut section, and another fault (240°/34°) was identified along the Sangu River section (figure 3). These two faults are parallel to the fold axis and longitudinally run through the western and eastern flanks. These faults are identified based on the abrupt change of bedding attitude data (mainly dip amount), locally exposed fault surface accompanied by fault-related deformation structures (e.g., discontinuity and visible displacement of the bedding, slickenside, breccia, shear bends, drag fold, fault bend folds), and sharp bends of the Sangu River course (along the eastern flank and northern plunge of the structure). All these features suggest that these two longitudinal faults are thrust faults (figure 4). In the Sangu River section, another set of faults is assumed to be present, which are inferred based on the straight

course of the river and the presence of deformation features at the sharp bands. These faults are roughly east–west oriented and approximately orthogonal to the two longitudinal faults. Hence, these faults can be named transverse faults. Due to insufficient field evidence, the nature of these faults is not clear.

The kinematic shear sense indicator related to the thrust-shear zone was observed during the field investigation in the Bandarban Anticline. This deformation zone is best preserved in the Boka Bil Formation, a thinly bedded shale unit with calcareous sandstone bands. Although thrust-shear zones are observed in different parts of the Bandarban Anticline, they are well exposed in the eastern flank along the upstream and downstream parts of the Sangu River section. In general, the thrust is west-dipping and east verging. The west-dipping high-angle thrust fault (265°/32°) cuts through gently dipping shale beds (070°/27°), produces a contractional duplex and gradually becomes horizontal in the up-dip direction at its end and produces a sigmoidal structure (figures 4 and 5c). Growth strata unconformity has been observed in the yellowish-brown poorly consolidated sandstone with trough and planar cross-bedding known as Tipam Formation exposed within the Bandarban University campus. The campus is located in the forelimb of the western flank along the Chittagong–Bandarban Road cut section (figure 5b). In the Sangu River section (downstream), several east-verging and west-dipping thrusts have been observed in the eastern flank of the Bandarban Anticline, which is probably the branch of a major thrust. The major thrust (240°/34°) is probably the northward continuation of the Sangu upstream thrust (figures 2 and 5a, e, f). A shear zone with a small thrust component has been observed in the eastern flank near the Bandarban Bus Stand area (figure 5a, e). The exposures on both sides of the road cut clearly show well-developed shear zones in the Boka Bil Formation dipping opposite to that of the bedding. The orientation of the exposure is EW and the photographs are taken facing N (figure 5e, f).

4.3 *Geometrical analysis of the bedding attitude data*

In the Bandarban Anticline, 83 bedding attitude measurements have been collected for the fold geometry analysis. In total, 54% of the measurements were taken from the western flank and the remaining 46% from the eastern flank of the structure. About 3% of the total measurements were taken from the overturned beds and are only used for density contouring for the determination of the pole of the flanks using Stereonet v.11 (Allmendinger *et al.* 2012; Cardozo and Allmendinger 2013). The poles to the bedding planes have been superimposed on the pole density contoured diagram, which was constructed using Kamb contour (Kamb 1959) with contour interval 2, significance 3, and the counting grid nodes resolution 30. Based on the mean contour value of each flank, a beta-diagram of both flanks has been prepared (figure 6). Based on the intersection of the east flank (243°/55°) and west flank (047°/37°), the fold axis (327°/8.5°) and interlimb angle (∼130°) of the fold have been determined. The stereographic analysis (figure 6) and mapping of the bedding orientation data (figure 3) reveal that the Bandarban structure is an asymmetric anticline. The orientation of the anticline is ∼327°, which is gently plunging (∼8.5°) to the north.

4.4 *Sedimentary facies analysis*

The facies that are identified in the Bandarban Anticline are summarized in (table 2) and their genetic relationships are shown in figures 7 and 8. These facies are categorized based on their lithologic characteristics because of the lack of any fossils and grouped into sandy- and muddy-lithofacies. They are further subdivided on the basis of textural properties, presence or absence of any sedimentary structure, bedform size, colour, the presence of clasts and their types.

4.5 *Facies associations*

The lithofacies identified in the Upper Bhuban, the Boka Bil, the Tipam Sandstones and the Dupi Tila formations of the Bandarban Anticline are grouped into three major facies associations: FA-1, FA-2 and FA-3 (figures 7 and 8).

FA-1: This facies association is found in the Upper Bhuban Formation of the Shaila Propat section, which comprises a thick, muddy sequence that is typically laminated to thinly bedded with silt streaks and lenses but occasionally massive bedded (figure 7a). The lithofacies found in this facies association are mudstone (C_m), mudstone with fine sand/silt streak (C_s), shale with fine sand/silt

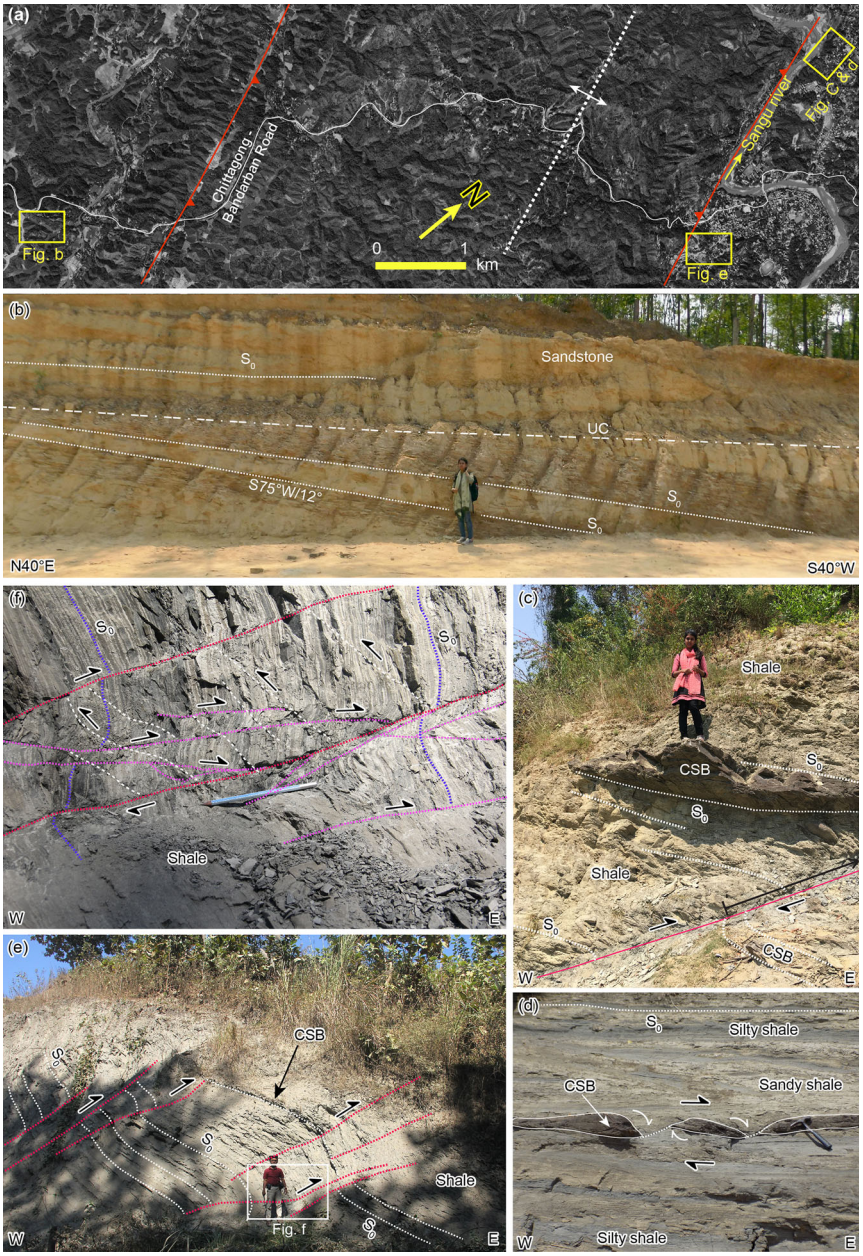

Figure 5. Structures observed in the Bandarban Anticline. **(a)** The Google Earth Pro panchromatic satellite image showing the Chittagong–Bandarban Road cut section. Faults are marked with red lines, and the axis is marked with white broken line. The yellow rectangles represent the locations of figure (b–e). **(b)** A local angular unconformity (white dotted line) separates subhorizontal beds (above) from gently tilted (S_0, S75°W/12°) strata below, and is interpreted to be a growth strata unconformity. **(c)** Geometry and kinematics of the west-dipping thrust, which shows a visible displacement (~1.5 m) of the calcareous sandstone band (CSB) on the opposite side of the fault plane. **(d)** The well-developed sigmoidal structure clearly indicates the top to the left (approximately eastward) shear movement just above an east-verging and west-dipping synthetic thrust. The hammer length in the picture is 0.30 m. **(e)** Shear bends with minor thrust components developed in the Boka Bil Formation. More than two shear bends with decimetre to centimetre scale displacement have east-verging (half arrow) and west-dipping shear plane. Along the shear plane, shale beds are highly compacted and are subjected to brittle-ductile deformation. Red dotted lines outline the shear planes, whereas white dotted lines outline the bedding planes (S_0). CSB: calcareous sandstone band. Rectangle marked the position of the latter figure (f). In the picture, the man is 1.64 m long. **(f)** Zooming of figure (e) demonstrates the well-developed shear planes (marked with red dotted lines) with two Riedel shear sets. The shear plane kinematics (marked with half arrows) is clearly marked by the curved, thin shale beds along the shear plane. The Reidel shear (R) and the antithetic Reidel shear (R') (Swanson 1988) are marked with white and pink dashed lines, respectively. Approximately east–west principal stress orientation (σ_1) can be inferred based on the orientation of the Reidel shear and the antithetic Reidel shear. The shear plane kinematics is marked with half arrows. The pencil length in the picture is 0.12 m.

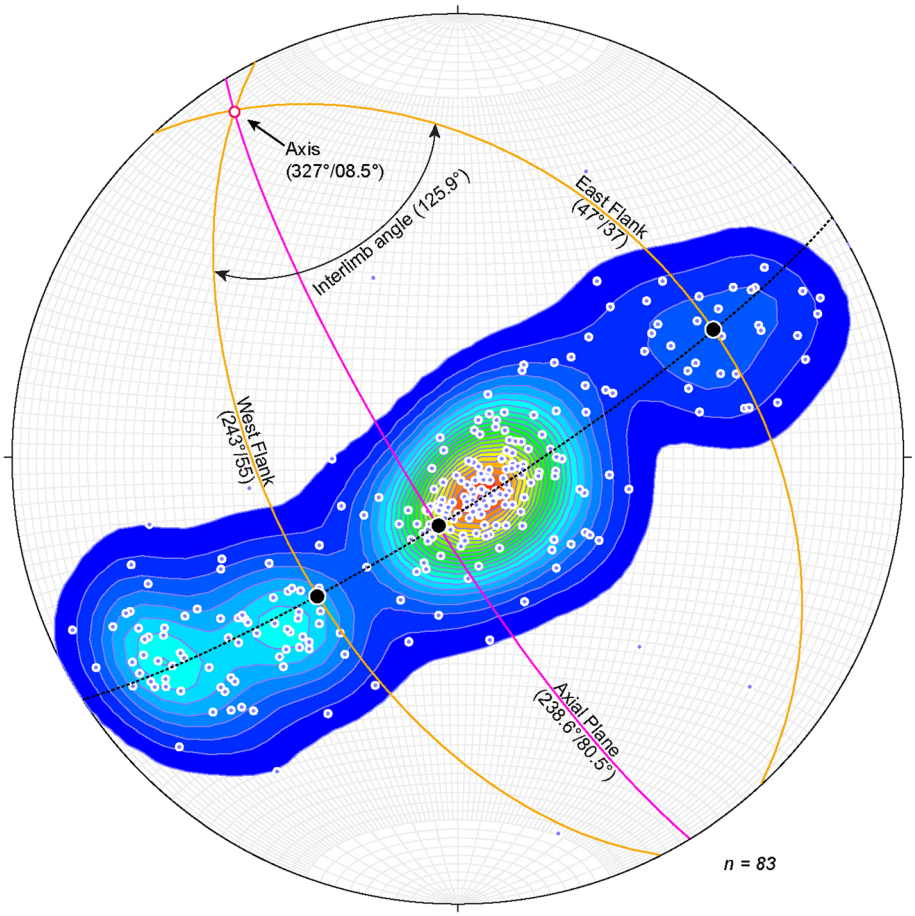

Figure 6. The stereographic analysis of the bedding orientation. The pole point diagram is superimposed on the pole density contour diagram. The data were measured from the road cut and river sections on both flanks of the Bandarban Anticline. The analysis reveals asymmetric, west-verging, north-plunging, and open fold nature.

lenses (Sh_{ls}), silty shale with fine sand/silt lenses ($SlSh_{ls}$), and mudstone with fine sand/silt lenses (C_{ls}) with occasional calcareous sandstone band (S_c) (figures 9a, b).

FA-2: This facies association is found mainly in the Boka Bil Formation of the Bandarban Anticline. In this facies association, different lithofacies such as sandstone (S), sandy shale (SSh), mudstone (C) and shale (Sh) occur alternatively and show different types of sedimentary structures of which lenticular-, wavy- and flaser-beddings are dominant. The FA-2 can be divided into three sub-facies associations: FA-2a, FA-2b and FA-2c (figure 7b–f).

The detail logs of exposures located at the Chittagong–Bandarban road cut section (figure 7b–d) and the Sangu River section (figures 7e, f) represent FA-2a. This sub-facies association is characterized by repeated fining-upward successions of flaser-bedded sandstone (S_f), wavy-bedded sandy shale (SSh_w) and lenticular bedded shale (Sh_{ln}) lithofacies (figures 9c–e) with occasional bedded mudstone (C_b), massive mudstone (C_m) and calcareous sandstone band (S_c) lithofacies (figure 9f). On the other hand, the sub-facies associations FA-2b and FA-2c occur in juxtaposition with FA-2a (figure 7b, d, e). The FA-2b comprises trough cross-bedded sandstone (S_t), which contains numerous mud clasts, especially at the erosion base of the lithofacies (figures 7e, 9g). Besides, the thick massive sandstone with mud clasts (S_{mc}) lithofacies in the Bandarban road cut section (figures 7b, 9h) is also considered to be a part of sub-facies association FA-2b as it contains numerous mud clasts. However, the FA-2c is found only in the Chittagong–Bandarban Road cut section (figure 7d), which consists of thick, massive sandstone lithofacies (S_m) (figure 9i).

FA-3: Only five lithofacies are identified in this facies association for which the facies code of Miall (1978) is used. These facies are trough cross-bedded sandstone (S_t), planar cross-bedded sandstone (S_p), ripple cross-laminated sandstone (S_r), alternation of

Table 2. *Summary table of lithofacies identified in the Neogene succession of the Bandarban Anticline, Chittagong–Tripura Fold Belt.*

Facies code	Lithofacies/ thickness (cm)	Sedimentary structures	Description	Interpretation
Sandy lithofacies				
S_t	Trough cross-bedded sandstone (∼20–100)	Trough cross-bedding	Fine to medium-grained, moderate to poorly sorted, yellowish-brown colour, some beds are gray coloured	Deposited due to migration of dunes during high energy condition (lower flow regime), such condition occurs mainly in both channel and bar
S_p	Planar cross-bedded sandstone (∼10–30)	Planar cross-bedding	Fine to medium-grained sandstone; yellowish-brown, poorly to moderately sorted; unconsolidated	Deposited due to lateral accretion of bars within channel
S_m	Massive sandstone (∼10–170)	Massive	Fine-grained massive sandstone; well sorted; light gray in colour	Formed through rapid deposition; internal structure of the sandstone beds might be destroyed due to weathering effect
S_{mc}	Massive sandstone with mud clasts (∼10–250)	Massive	Fine- to medium-grained, massive sandstone; light gray in colour; moderately sorted; have numerous mud clasts	Also formed through rapid deposition; presence of mud clasts indicates erosion of previously deposited clay/mud beds due to high energy current flow which transported these clasts and then redeposited when flow velocity decreased; such condition occurs mainly in channel
S_f	Flaser-bedded sandstone (10–25)	Flaser-bedding	Fine to very fine-grained, light gray sandstones; matrix dominating; muds are deposited on ripple troughs forming flaser-bedding	Formed in lower intertidal to subtidal zone where current velocity is generally high (lower flow regime condition), that leads to the migration of sand ripples; because of periodic breaks in the current flow, muds were deposited as streaks within sand ripples
S_r	Ripple cross-laminated sandstone (∼20)	Ripple cross-lamination	Fine- to very-grained, moderately sorted, yellowish sandstone; asymmetric ripples	Deposited in lower flow regime conditions where moderate flow velocity allowed the migration of current ripples
S_c	Calcareous sandstone (∼5–10)	Mainly structureless; occasionally low angle cross-laminated	Fine- to very fine-grained, light gray, calcareous sandstone band; very hard and compact	Cross-lamination were formed due to migration of current ripples; but in most cases, sandstone are highly cemented that destroyed the depositional structures
Muddy lithofacies				
Sh_l	Shale (∼5–30)	Lamination	Gray colour; fine sand/silt streaks are present	Intermittent deposition of mud in low energy condition that allow settling of suspended fine sediments
Sh_{ls}	Shale with fine sand/ silt lenses (∼10–80)	Lamination; fine sand/silt lenses	Dark grey shale with discontinuous to continuous fine sand/silt thin lenses, highly bioturbated	Settling down of suspended loads in calm water periods; whereas the lenses of fine sand/silt were formed due to migration of ripples during intermittent low energy current flow; suitable condition for living of burrowing organisms.

Table 2. *(Continued.)*

Facies code	Lithofacies/ thickness (cm)	Sedimentary structures	Description	Interpretation
Sh_{ln}	Lenticular-bedded shale (∼10–20)	Lenticular-bedding	Gray to light gray colour shale with thin, fine sand to silt lenticles/lenses. Most lenses are of various dimensions and both isolated and weakly connected in nature	Formed in tidal environment, especially supratidal zone, where mud deposited on top of ripples during periods of slack water. Mud dominating low energy depositional system
SSh_w	Wavy-bedded sandy shale (∼5–12)	Wavy-bedding	Gray colour sandy shale; sand lenses are connected to each other formed thin cross lamination	Formed in tidal environment (intertidal zone), where both mud and sand were available; mud deposited during slack-water period, whereas cross-laminated sand formed due to migration of ripples during flows of tidal current
$SlSh_{ls}$	Silty shale with fine sand/silt lenses (∼10)	Lamination, fine sand/silt lenses	Gray colour silty shale with relatively thick fine sand/silt lenses, some are continuous	Deposited from mixed-load suspension; intermittent low energy condition
C_m	Mudstone (∼15)	Massive	Dark gray colour mudstone with no internal structure	Continuous deposition of mud due to suspension settling in low energy condition
C_b	Bedded mudstone (∼20)	Bedding	Bluish gray, thickly bedded mudstone; argilaceous	Intermittent deposition of mud due to suspension settling in low energy condition
C_s	Mudstone with fine sand/silt streak (∼50–80)	Massive	Dark gray colour mudstone with discontinuous fine sand/silt streak; bioturbated	
C_{ls}	Mudstone with fine sand/silt lenses (∼20–40)	Thinly bedded fine sand/silt lenses	Dark gray mudstone; contain fine sand/silt lenses which are not connected to each other; bioturbated	Suspended loads deposition in calm waters; intermittent flow of currents caused the migration of ripples forming the isolated fine sand/silt lenses
F_l	Alternation of laminated mud and fine sand (∼40)	Lamination	Finely laminated mud with very fine sand interlaminae; mud layers are gray coloured, whereas sand layers are yellowish-brown; sand layers are structureless	Settling of suspended loads with intermittent very weak current flow; probably deposited on bar top and subordinately on flood plain; depositional structure in sand layers is hard to identify due to weathering
F_m	Massive mud	Massive	Dark gray to bluish gray mud, mostly structureless, occasionally shows fine lamination	Settling of suspended loads in prolonged calm water condition over flood plains

laminated mud and fine sand (F_l), and massive mud (F_m) (figure 8). This facies association is found in the Tipam and the Dupi Tila formations.

Dominant lithofacies in the Tipam Formation are S_t and S_p (figures 10a, b) with minor intercalation of F_m facies. These sandstone deposits are moderately sorted and contain numerous clay galls (figure 10c), some of which are several centimetres in diameter (figure 10d). The overall succession shows several fining upwards sequences in which erosion surfaces are identified at the bases of facies S_t; relatively fine-grained lithofacies S_p are deposited over it and both these facies are sometimes separated by thin F_m facies (figures 8a, b).

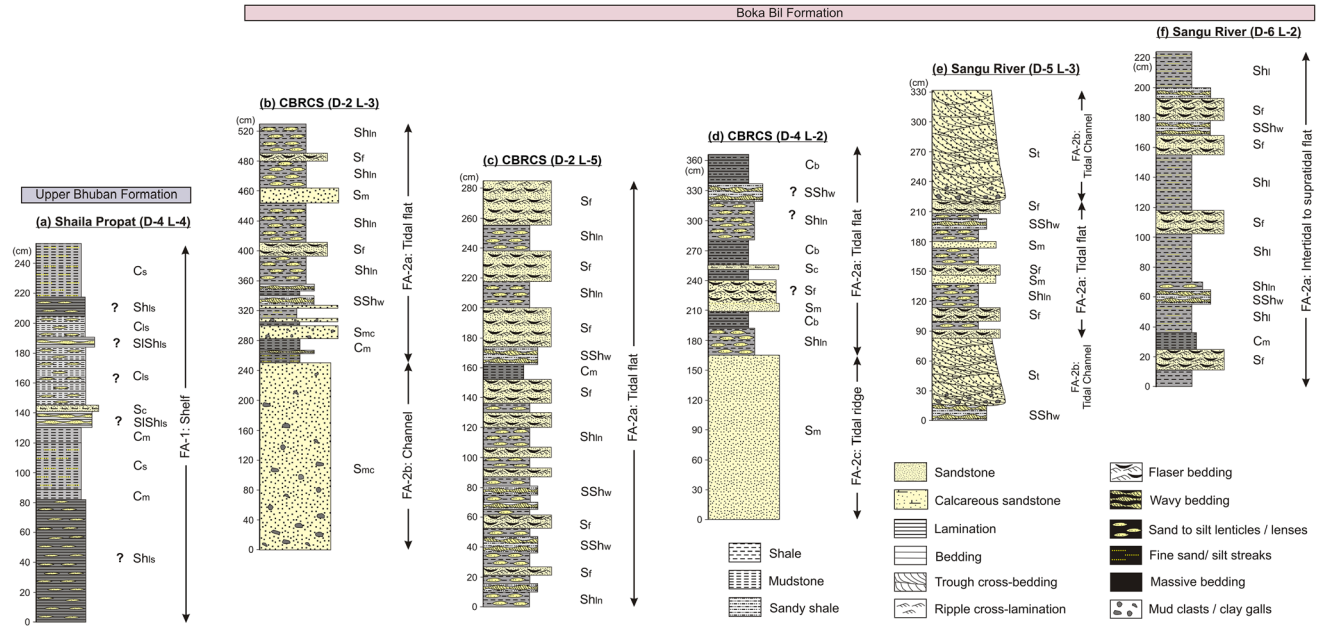

Figure 7. Detailed sedimentological logs of the Bhuban and the Boka Bil formations from the Bandarban Anticline showing characteristic lithology, texture, sedimentary structures, and lithofacies. The right-marginal column shows the possible genetic interpretation of facies associations. See table 2 for the explanation of lithofacies. Lithofacies that are difficult to identify are marked by question marks. CBRCS: Chittagong–Bandarban Road cut section.

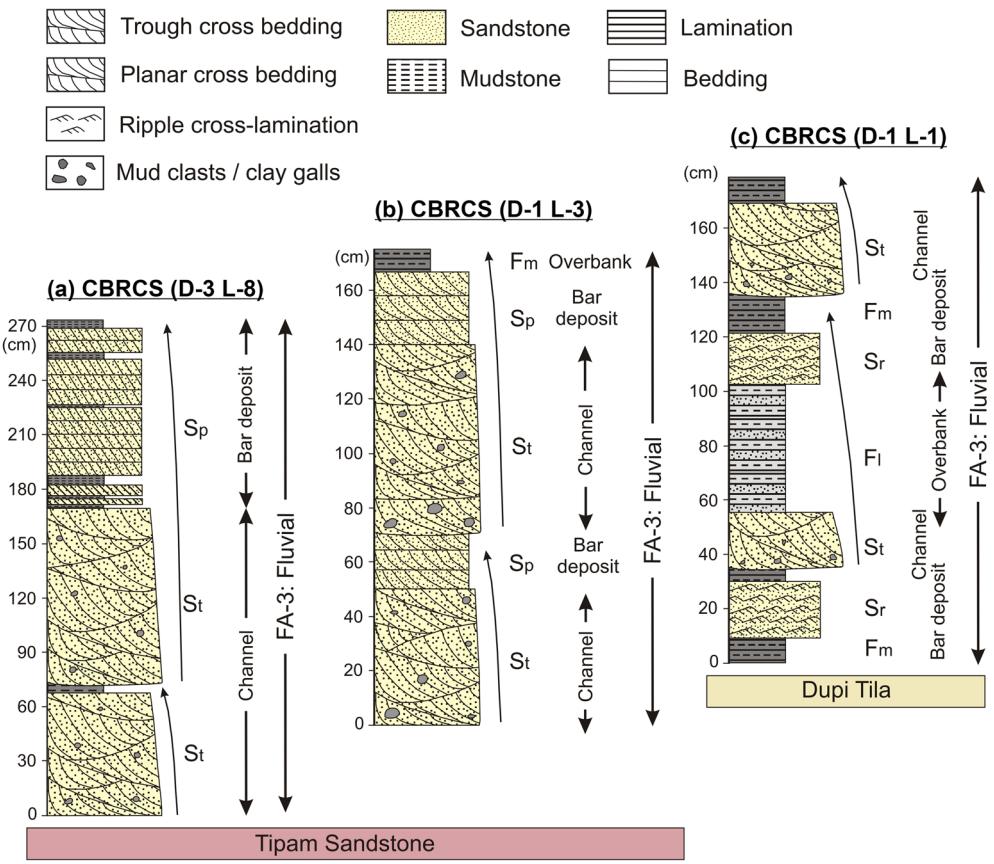

Figure 8. Vertical lithologs showing lithology, sedimentary structures, and vertical grain size trends of the Tipam and Dupi Tila formations in the Bandarban Anticline.

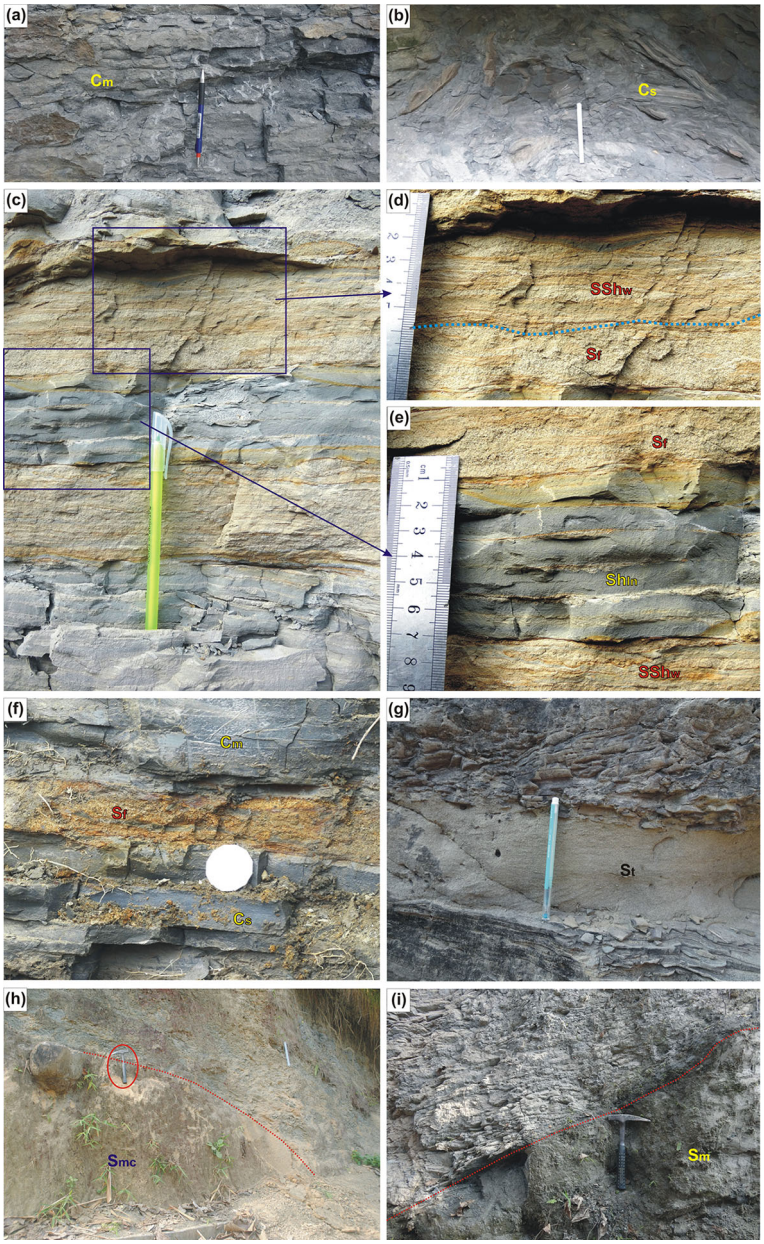

Figure 9. Photographs showing lithofacies of the Bokabil and the upper Bhuban formations of the Bandarban Anticline: **(a)** Mudstone (C_m) facies in the Shaila Propat section. **(b)** Mudstone with fine sand/silt streak (C_s) facies in the Shaila Propat section (35 cm long hammer for scale). Both C_m and C_s are highly deformed due to tectonic activity. **(c–e)** Lenticular-bedded shale (Sh_{ln}) facies, wavy-bedded sandy shale (SSh_w) and flaser-bedded sandstone (S_f) facies in the Chittagong–Bandarban Road cut section (in Meghla Tourist Complex). **(f)** Flaser-bedded sandstone (S_f) lithofacies in between massive mudstone (C_m) and bedded mudstone (C_b) facies in the Chittagong–Bandarban Road cut section. Coin (2.5 cm diameter) for scale. **(g)** Tidal channel with trough cross-bedded sandstone (S_t) and overlying tidal flat deposits at the Sangu River section. 15 cm long pen for scale. **(h)** Massive sandstone with mud clasts (S_{mc}) lithofacies which is overlaid by tidal flat deposits at the Chittagong–Bandarban Road cut section (location of sedimentological log in figure 3). 35 cm long hammer for scale. **(i)** Sharp contact between massive sandstone (S_m) lithofacies and tidal flat deposits (location of sedimentological log in figure 3). Hammer (35 cm) for scale.

On the other hand, this facies association in the Dupi Tila Formation is mud dominant. Detail log of location-1 at the Chittagong–Bandarban Road cut section (figure 8c) shows two prominent erosion surfaces above which small-scale trough cross-bedded sandstones (S_t) with mud clasts are deposited (figure 10e). These trough cross-bed sets are several centimeters thick. Two isolate beds of facies S_r occur within fine-grained facies, i.e., F_l and F_m lithofacies (figure 8c).

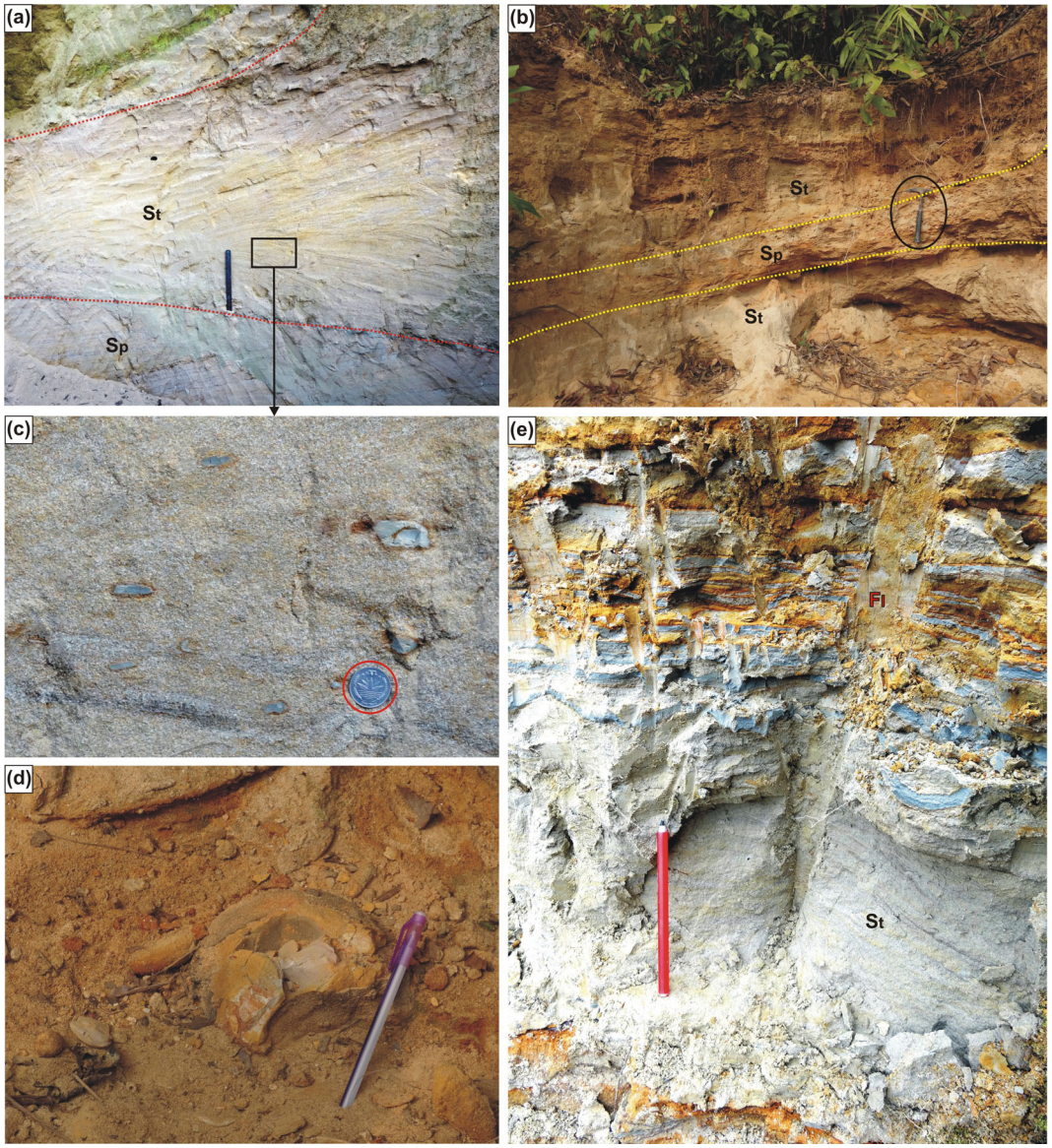

Figure 10. The lithofacies in the Tipam and the Dupi Tila formations at the Bandarban Anticline: **(a)** Large trough cross-bedded sandstone (S_t) overlaying the planar cross-bedded sandstone (S_p) at the Chittagong–Bandarban Road cut section. 30 cm ruler scale for image scale. **(b)** Trough cross-bedded sandstone (S_t) and planar cross-bedded sandstone (S_p) at the Chittagong–Bandarban Road cut section. Hammer for scale (35 cm long). **(c)** Clay galls found in lithofacies S_t at the Chittagong–Bandarban road cut section. Coin for scale (2.5 cm). **(d)** Large clay gall (∼15 cm diameter) in S_t lithofacies at the Chittagong–Bandarban Road cut section. **(e)** Trough cross-bedded sandstone lithofacies (S_t) overlaying by the alternation of laminated mud and fine sand (F_l) at the Chittagong–Bandarban Road cut section. These lithofacies are found in the lower Dupi Tila Formation.

5. Discussion

5.1 *Surface geology and structure*

The Bandarban Anticline (figure 1b) is situated approximately in the middle of the CTFB, which is an NNW–SSE oriented anticline developed through buckling and fault propagation folding in mechanically heterogeneous layered of Neogene sediments (Das *et al.* 2022; Hossain *et al.* 2022). This younger western IBR fold-thrust belt formed as an accretionary wedge linked to the hyper-oblique convergence of the Indian and Burmese plates and has been dated at ∼2 Ma and continues to the present day (Maurin and Rangin 2009; Najman *et al.* 2012; Oryan *et al.* 2023). Hence, the present-day surface geology and geomorphology of this area reflect the equilibrium between tectonic uplift, erosion, and alluvial deposition (Khan *et al.* 2018). Anticlinal ridges, linear valleys, and streamlet/river, particularly the incised Sangu River, are the significant geomorphic features of the study area.

Hill slopes of the study area are controlled by tectonics and, in turn, control the stream network. The area is traversed by a dendritic drainage network of small streams and streamlets/chara. Stream morphological attributes (i.e., initiation of new streams, convergent drainage, offset streams and scarps, and breaks in slope) seem to be formed either due to the fault or lithological changes (figure 2). Linear features are drawn on the drainage map based on the stream morphological attributes and then cross-checked with the surface geology (lithology as well as structures), as shown in figure 3. In most cases, the linear features drawn in figure 2 coincide with the geological boundaries (either lithological or structural, figure 3). Two major longitudinal and few transverse faults are seemed to be thrust and strike-slip faults, respectively, as indicated by surface deformation features (figures 4 and 5). Additionally, the antecedent Sangu River (Valdiya 1996; Fryirs and Brierley 2010) is most likely structurally controlled, as indicated by the field and satellite remote sensed observations. Observed deformation structures along the seven sharp bends of the Sangu River in the eastern flank and northern plunge of the Bandarban Anticline suggest that the NNW–SSE and W–E orientated faults are mainly thrust and strike-slip faults, respectively. The fault orientation (figure 3) and their related deformation kinematics (figures 4 and 5) are well constrained by the orientation of the regional maximum compressive stress (approximately E–W to ENE–WSW directed compression) of the CTFB (Angelier and Baruah 2009; Betka *et al.* 2018; Hossain *et al.* 2022). The linear valley that has been observed in the western flank along the Chittagong–Bandarban Road cut section, which overlaps with field-indented thrust fault, possibly suggests the presence of a strike-slip component of this thrust (Replumaz *et al.* 2001; Duvall and Tucker 2015; Khan *et al.* 2018). Therefore, it is clearly evident that for accurate identification of the lithological boundaries as well as structural features in the field, systematic interpretation of the base observed geomorphic features can be used as an important guided tool.

The stereographic analysis of the bedding attitude data demonstrates that the orientation of the axis of the anticline is ∼327° with a gentle plunging (∼8.5°) to the north (figure 6). However, it is worth mentioning here that this dataset is collected along the two sections (i.e., road cut and Sangu River), which are approximately from the northern part of the structure. Hence, it is impossible to comment on whether the structure is plunging to the south. The analysis also reveals that the Bandarban Anticline is asymmetrical with an axial surface orientation (i.e., dip direction and dip amount) of 239°/81° and an interlimb angle of 126°. The longitudinal thrusts in the western flank are west-verging and east-dipping, which are the direct result of Indian and Burmese plate collisions and are the dominant thrust system of the area. The thrust in the eastern flank is west-dipping and east-verging. As the west-dipping thrust has vergence opposite the dominant trend of a thrust system, this thrust is designated as the back thrust of the west-verging master thrust. Most of the compressional stress and associated strain has been taken up by movement along these thrusts,

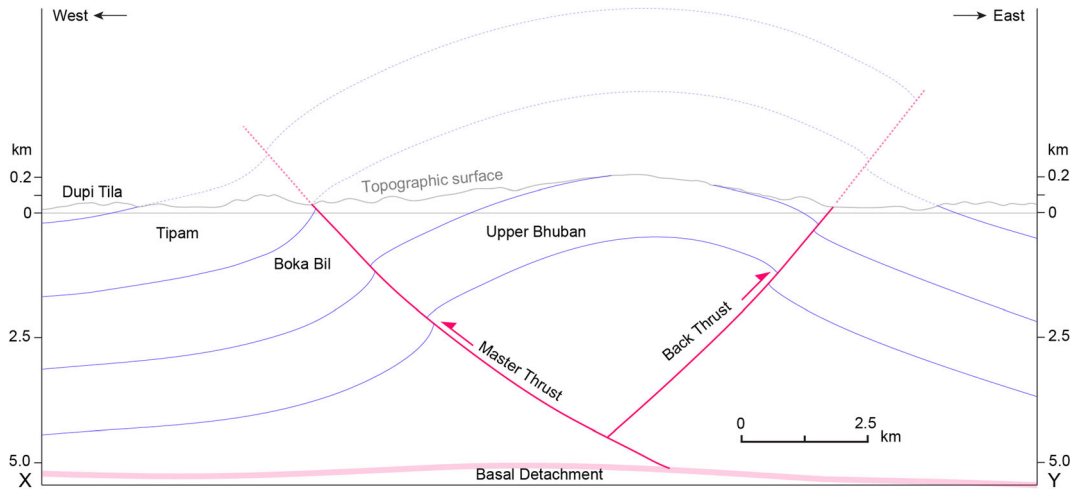

Figure 11. Schematic 2D structural model along the line XY – the Chittagong–Bandarban Road cut section (position of the line XY is shown in figure 3). Note: The purple lines are the lithological boundaries, and the solid red lines are the thrust.

resulting in wedge-shaped upliftment of the central part, possibly due to cessation of the propagation along the decollement, but displacement on the thrust behind the fault tip is continuing. The 2D structural model/cross-section of the structure (figure 11) is constructed based on the detailed geological field observations and measurements (figures 3–5) along the Chittagong–Bandarban Road cut section and clearly reflects the nature of the anticline (i.e., fault propagating fold).

Tectonically, the Bandarban Anticline is located at the central portion of the folded flank of the Bengal Basin (i.e., CTFB, figure 1b) (Hossain *et al.* 2022). The structure is amalgamated with the Mowdak structure in the southern part and continues to the Myanmar terrain in the south. As of the majority of the CTFB anticlines (Sikder and Alam 2003; Mandal *et al.* 2004; Maurin and Rangin 2009; Najman *et al.* 2012; Betka *et al.* 2018; Khan *et al.* 2018; Burgi *et al.* 2021; Hossain *et al.* 2022), both flanks of this structure are faulted, and these faults mostly accommodated dip-slip thrust components and trifling strike-slip components. Kinematic analyses of the Bandarban Anticline suggest that this structure results from east-directed subhorizontal shortening, which is orthogonal to the fold axial plane. Extensive paleostress analysis of the CTFB structures by Hossain *et al.* (2022) revealed no evidence of substantial strike-slip faulting or transpression. Hence, the measured approximately E–W shortening orientation based on the fault's kinematics (figures 4 and 5) is consistent with the maximum horizontal stress orientations derived from the absolute plate motion direction and earthquake focal mechanism solutions by Hossain *et al.* (2022). Recent geodynamic observations suggest that subduction in this region is active (Gahalaut *et al.* 2013; Heidbach *et al.* 2016; Steckler *et al.* 2016; Mallick *et al.* 2019). A few moderate and one-large magnitude earthquakes have been recorded in the CTFB region (Hossain *et al.* 2019). The Bandarban earthquake in 1997 (M_w 6.1) is well-known among these earthquake events. Surface geomorphology, geodynamic observations, and earthquake occurrence suggest that the Bandarban Anticline and its surrounding structures are tectonically active.

5.2 *2D structural model of the study area*

A 2D structural model or the geological cross-section has been constructed (figure 11) along the Chittagong–Bandarban road cut section based on the satellite imagery, drainage morphology (figure 2), surface geology, bedding attitude data, and fault locations based on the fieldwork (figure 3), and extracting regional structural style from the previous investigations (Sikder and Alam 2003; Steckler *et al.* 2008; Maurin and Rangin 2009; Hirschmiller *et al.* 2014; Khan *et al.* 2018; Burgi *et al.* 2021; Hossain *et al.* 2022). Careful field investigation suggests that the folds and thrust faults have been developed concurrently or at later times, which is similar to the regional structural styles. Structural styles from 2D seismic sections in nearby structures also suggest similar results. Both flanks of the structure are thrusted and dip towards the core of the structure and are connected to lower detachment. The location of the thrusts, their dips, and vergence are determined based on the fault attitude, kinematic interpretation of the deformation features, and drainage morphological features.

5.3 *Paleoenvironmental reconstruction*

The lithofacies characteristics and their corresponding facies associations found in the upper Bhuban, the Boka Bil, the Tipam Sandstones and the Dupi Tila formations of the Bandarban Anticline give evidence of deposition of the sedimentary sequence from shallow marine shelf (FA-1) through marginal marine tide dominating delta (FA-2) to continental fluvial (FA-3) depositional settings (figures 7 and 8), suggest a basinward progradation of this Neogene succession. Some authors (e.g., Haque and Roy 2021; Huq *et al.* 2000) suggest that the exposed sedimentary sequences of the Bandarban Anticline are turbidite deposits of submarine fans. However, observations of this study strongly suggest progressive deposition of these sediments in the continental shelf−tide dominating delta–fluvial depositional environments. However, there is a possibility to find the turbidite sequence in the lower Bhuban Formation, which is not exposed in the study area, but such type of submarine fan deposits was observed in the equivalent lower Bhuban Formation of other structures of the Chittagong–Tripura Fold Belt (Gani and Alam 1999, 2004).

The continental shelf deposits are represented by the mud dominating facies association FA-1 (figure 7a). Such type of facies association is also reported by Gani and Alam (1999) in the nearby Sitapahar Anticline of the CTFB. However, the lack of cross-bedding and hummocky cross-stratification suggest that this sequence was deposited in

the mid to deeper part of the shelf below storm wave-base where muddy sediments were deposited in low energy conditions due to suspension settling, but intermittent current flow caused the migration of ripples, those were preserved as lenses. However, some of the lithofacies were difficult to identify due to tectonic deformation, as the Shaila Propat section is located at the axial zone of the anticline (figure 3). On the other hand, the existence of flaser-bedded sandstone (S_f), wavy-bedded sandy shale (SSh_w) and lenticular bedded shale (Sh_{ln}) lithofacies in the overlying facies association FA-2 reflects tidal current influence depositional environment where repeated, small-scale alternations in sediment transport conditions prevailed (e.g., Alam 1995; Gani and Alam 1999; Boggs 2006). This facies association consists of different subenvironments such as tidal flat (FA-2a), tidal channel (FA-2b) and tidal ridge (FA-2c) of a tide-dominating delta (figures 7b–f, 12a) in which these subenvironments occurred side by side and overlap each other with local sea level fluctuations.

In tidal flat, the flaser-bedded sandstone (S_f) units are deposited in lower intertidal to upper subtidal zones, whereas mud and fine sand-dominated wavy-bedded sandy shales (SSh_w) are interpreted as intertidal deposit. The mud-dominated lenticular bedded shale (Sh_{ln}) represents the upper intertidal zone, which was intermittently merged with the supratidal marsh of the tide-dominated delta. Such a feature is observed in the Sangu River section (figure 9g), where predominant shale (Sh_l) lithofacies could be deposited in low-energy supratidal zone. The cyclic occurrences of sub-, inter-, and supratidal deposits suggest that these lithofacies were deposited during repeated cycles of

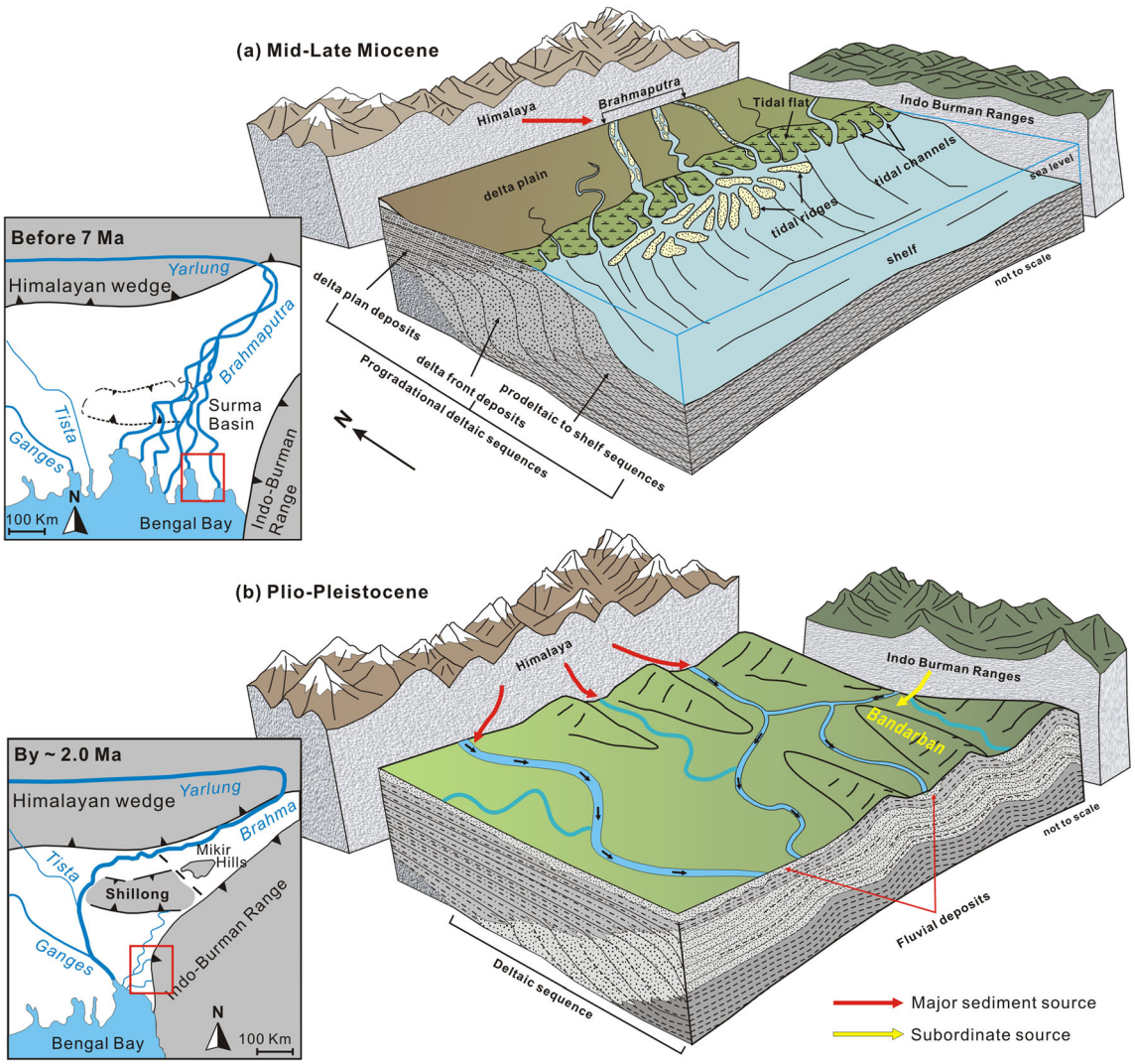

Figure 12. Generalized models for the tectonosedimentary evolution of the Bandarban Anticline and its adjoining areas (marked by red box in indexed figures which are after Govin *et al.* 2018): (**a**) during Mid-late Miocene and (**b**) during Pliocene-Pleistocene. Sea-level fluctuations during deposition of these sedimentary sequences were not considered in this model.

progradation (Boggs 2006). In contrast, the occurrences of trough cross-bedded sandstone (S_t) in the Sangu River section (figures 7e, 9g) suggest deposition most likely in tidal channels, which occurred in juxtaposition with tidal flat deposits. This lithofacies contains numerous mud clasts, especially near the erosional surface of the channel. However, the thick, massive sandstone with mud clasts (S_{mc}) lithofacies in the Bandarban road cut section (figures 7b, 9h) can also be interpreted as channel deposits. These mud clasts were formed by erosion of previously deposited mud or clay beds due to high energy current flow, which also transported these clasts and then redeposited when flow velocity decreased. Deposition of lithofacies S_t and S_{mc} is followed by the tidal flat deposits (e.g., lithofacies Sh_{ln}, SSh_w, S_f and C_m), which suggest shifting of the channel and producing a fining-upward sequence (figures 7b, e). However, the identification of an appropriate depositional condition of thick massive sandstone lithofacies (S_m) in the Boka Bil Formation (figures 7d, 9i) is difficult due to the lack of internal structure, but fine-grained and fairly well-sorted characteristics and co-occurrence with tidal flat facies association indicate that they are probably formed in tidal sand ridges/bars of tidal-dominating delta depositional settings.

With delta progradation, a fluvial depositional environment was established, which is suggested by facies association FA-3 (figure 8). In the Tipam Sandstone, the FA-3 is sand dominant and shows several fining upwards sequences (figure 8a, b), which hints at the deposition by multi-channelled braided river system. The vertical stacking of bar deposits is the result of multiple episodes of channel shifting and bar migration in braided rivers (Miall 1996; Boggs 2006). In contrast, mud-dominant FA-3 in the Dupi Tila Formation (figure 8c) suggests a meandering river depositional setting. Such types of deposits are also reported in the Dupi Tila Formation of the Sylhet Trough, which was deposited by a meandering river system (Gani and Alam 2004). In this case, decreasing flow velocity produced the fining upward cycles, and both channel and bars are confined within thick flood plain deposits.

6. Tectonostratigraphic evolution

Geomorphology, geological field mapping, structural observations, fold geometry, and deformation kinematics suggest that the Bandarban Structure is an asymmetric, west-verging, high-amplitude anticline that is gently plunging to the north (figure 6). To the east and west, two major N–S trending high-angle reverse faults have been identified running almost the entire length of the structure based on the presence of abrupt change in bedding dip amount, discontinuity of the bedding, major drainage offset, linear valleys and ridges, and fault-related deformation structures (figures 4 and 5). However, previous studies (Haque and Roy 2021 and references therein) did not report these two major faults of the Bandarban Anticline. The tectonostratigraphic evolution of the study area broadly divided into two stages: stage 1 is the deposition of the sediments in the Bandarban Anticline and its adjacent areas, and stage 2 is the development of the Bandarban Anticline as a part of the CTFB during India–Burma collision. A simplified tectonostratigraphic evolution model of the Bandarban Anticline proposed in this study is shown in figure 12.

Stage 1: Sedimentation in the present Bandarban Anticline and its adjoining areas was the consequence of the gradual filled-up of the Bengal Basin by the progradation of the delta over shelf deposits (figure 12a). The thick deltaic sequence of the area suggests that these were deposited prior to any tectonic deformation. The principal sediment source of this deltaic sequence was the rising Himalaya since the paleo-Brahmaputra flowed directly south-southwest and transported Himalayan sediments to the Bengal Basin (Govin *et al.* 2018). However, the consequences of delta progradation and the gradual fall of eustatic sea level during the Pliocene–Pleistocene, a fluvial dominating depositional settings, were established in the study area where the Tipam Formation began to be deposited.

Stage 2: Pliocene-Pleistocene-Recent tectonostratigraphic evolution of the Bandarban Anticline was controlled by the origin and development of two major reverse faults and the glide along the major basal decollement (figure 6) and was possibly directly associated with the westward propagation of the outer Indo-Burmese wedge due to the subduction of the Indian Plate beneath the Burmese Plate. The latest episode of structural activation, which creates the folding in the outer Indo-Burman wedge (i.e., CTFB), has possibly occurred during or immediately after the deposition of the Tipam Formation (i.e., during the Pliocene-Pleistocene). After the initial development of the fold and its subaerial exposures, the strata were subjected to

dominant brittle rock deformation and activated the in-sequence thrust and back thrust in the forelimb and backlimb, respectively. These reverse faults resulted in a rapid uplift of the Bandarban Anticline, which was subsequently subjected to erosion due to convergence tectonics from the Late Pleistocene to Recent. The continued collision-related tectonic uplift and consequent erosion are also coeval with the last glaciation maxima-induced eustatic sea level fall during the Late Pleistocene. The Bandarban Anticline, which is situated in the middle of the CTFB area, is subjected to the approximately E–W compressional force resulting from the Indo-Burmese hyper-oblique collision (Mitchell 1993; Maurin and Rangin 2009; Westerweel *et al.* 2019; Najman *et al.* 2022). Resultant rapid westward propagation of the outer IBR and coeval uplift of the Shillong Plateau as a pop-up structure closed and shifted the SSW-directed paleo-Brahmaputra course to its present west-directed course (figure 12). Consequently, the sediment supply, which was dominantly from the Himalayan region in the north through paleo-Brahmaputra is then taken by the rapidly rising Indo-Burman Ranges to the east (Govin *et al.* 2018; Rahman *et al.* 2020; Yang *et al.* 2020; Najman *et al.* 2022). Due to highly oblique Indian–Burmese plate active convergence, there is substantial strain partitioning between the number of crustal faults in the forearc and backarc (e.g., Steckler *et al.* 2016; Mallick *et al.* 2019). The strain partitioning results in purely convergent motion in the Western Outer IBR Belt (e.g., CCF), while the dextral strike-slip motion is concentrated in the eastern IBR and beyond (e.g., the Kaladan, Kabaw, Sagaing faults) (Maurin and Rangin 2009; Morley *et al.* 2020; Hossain *et al.* 2022). These observations are consistent with our study as there is scarce direct field evidence of strike-slip motion observed during this study in the Bandarban Anticline.

7. Conclusions

The CTFB, which includes the study area of the Bandarban Anticline, is the outer wedge of the IBR bounded by the Kaladan Fault and the CCF to the east and west, respectively. The Bandarban Anticline, as deduced from geomorphological analysis, geological field mapping, structural observations, fold geometry, and deformation kinematics, exhibits characteristics of an asymmetric, west-verging anticline, which is gently plunging to the north. Measured fault kinematics suggest approximate east–west shortening consistent with the previously published maximum horizontal stress orientations derived from the absolute plate motion direction and earthquake focal mechanism solutions. A number of lithofacies have been identified from the exposed rock formations and are grouped into three major facies associations: shelf/shallow marine (FA-1; Lower Boka Bil/Upper Bhuban Formation), tide dominating delta (FA-2; Boka Bil Formation), and fluvial (FA-3; Tipam and Dupi Tila formations). The study area, along with the CTFB as a whole, experienced different depositional settings temporally and spatially. From the exposed stratigraphic and structural evidence, it can be concluded that during the deposition of the Lower Boka Bil/Upper Bhuban Formation, the area was under the continental shelf setting. With the progression of time, the area converted into a tide-dominated delta setting during the deposition of the rest of the Boka Bil Formation. Because of the continued tectonics and/or sea level fall, the area uplifted significantly, and the Tipam and the Dupi Tila formations were deposited under fluvial settings. A tectonostratigraphic evolution model of the Bandarban Anticline is proposed, indicating sedimentation initially driven by delta progradation from the rising Himalaya and later from the IBR. Therefore, tectonostratigraphic evolution during the Pliocene-Pleistocene-Recent was controlled by the origin and development of Kaladan and CCF and the glide along the major basal decollement and was possibly directly associated with the westward propagation of the outer IBR. This late-stage tectonics initially develops fold in the area and later developed the longitudinal and transverse faults with the intensified tectonics.

Acknowledgements

We would like to thank the undergraduate and research students who accompanied and helped us in collecting primary data in the remote field area. The study is financially supported by the Jahangirnagar University Research Grants through the Faculty of Mathematical and Physical Sciences (Grant No. 2021–2022). The authors would like to thank the anonymous reviewers for the helpful comments and corrections and the Associate Editor, Dr George Mathew, for handling the manuscript and editorial input. The manuscript has greatly improved by comments from the reviews.

Author statement

Md Sakawat Hossain: Fieldwork, data analyses, draft writing, and finalizing the manuscript; Rumana Yeasmin: Fieldwork, data analyses, facies coding, and draft writing; Md Sharif Hossain Khan: Fieldwork, data analyses, and review of the draft; Md Ibna Reday: Fieldwork, data analyses, and figure drafting; Fatema Tuz Zohora and Samiya Tasnim Toma: Fieldwork, data analyses, and draft writing.

References

Alam M K and Quraishi A A 1985 Geology of Rawangchari–Ruma area, Bandarban District, Bangladesh; *Records Geol. Surv. Bangladesh* **3(4)** 1–15.

Alam M K, Hasan A K M S, Khan M R and Whitney J W 1990 Geological Map of Bangladesh, Scale 1:1,000,000; *Geol. Surv. Bangladesh*.

Alam M 1989 Geology and depositional history of Cenozoic sediments of the Bengal Basin of Bangladesh; *Palaeogeogr. Palaeoclimatol. Palaeoecol.* **69** 125–139, https://doi.org/10.1016/0031-0182(89)90159-4.

Alam M M 1995 Sedimentology and depositional environments of the Bengal Basin sub-surface Neogene succession based on the detailed facies and electrofacies analysis: A case study of the Kailash Tila, Rashidpur and Bakhrabad structures in northeastern Bangladesh; Ns. Coopera. Norad Project BGD-023, pp. 1–74.

Alam M, Alam M M, Curray J R, Chowdhury M L R and Gani M R 2003 An overview of the sedimentary geology of the Bengal Basin in relation to the regional tectonic framework and basin-fill history; *Sediment. Geol.* **155** 179–208.

Allmendinger R W, Cardozo N and Fisher D 2012 *Structural geology algorithms: Vectors and tensors in structural geology*; Cambridge University Press, 302p.

Angelier J and Baruah S 2009 Seismotectonics in Northeast India: A stress analysis of focal mechanism solutions of earthquakes and its kinematic implications; *Geophys. J. Int.* **178** 303–326, https://doi.org/10.1111/j.1365-246X.2009.04107.x.

Bakhtine M I 1966 Major tectonic features of Pakistan: Part II; *The Eastern Province Sci. Ind.* **4** 89–100.

Bangladesh National Building Codes 2020 Housing and Building Research Institute, Dhaka, Bangladesh; VI, CH 2:3185-3197.

Betka P M, Seeber L, Thomson S N, Steckler M S, Sincavage R and Zoramthara C 2018 Slip-partitioning above a shallow, weak décollement beneath the Indo-Burman accretionary prism; *Earth Planet. Sci. Lett.* **503** 17–28, https://doi.org/10.1016/j.epsl.2018.09.003.

Boggs S 2006 *Principles of Sedimentary and Stratigraphy;* Pearson Education, Inc., 662p.

Boruah A, Verma S, Rasheed A, Gairola G H and Gogoi A 2022 Macro-seepage based potential new hydrocarbon prospects in Assam-Arakan Basin, India; *Sci. Rep.* **12** 2273, https://doi.org/10.1038/s41598-022-06045-6.

Brammer H 2012 *The Physical Geography of Bangladesh*; University Press Ltd., Dhaka, 547p.

Brammer H 2014 Bangladesh's dynamic coastal regions and sea-level rise; *Clim. Risk Manag.* **1** 51–62, https://doi.org/10.1016/j.crm.2013.10.001.

Bürgi P, Hubbard J, Akhter S H and Peterson D E 2021 Geometry of the décollement below eastern Bangladesh and implications for seismic hazard; *J. Geophys. Res.: Solid Earth* **126** e2020JB021519.

Cardozo N and Allmendinger R W 2013 Spherical projections with OSXStereonet; *Comput. Geosci.* **51** 193–205.

Chowdhury K R, Hossain M S and Khan M S H 2022 Introduction to Bangladesh Geosciences and Resources Potential; In: *Bangladesh Geosciences and Resources Potential* (eds) Chowdhury K R, Hossain M S and Khan M S H, 1st edn, CRC Press, Taylor & Francis, USA, pp. 1–23, https://doi.org/10.1201/9781003080817.

Dahlstorm C D A 1969 Balanced cross sections; *Canadian J. Earth Sci.* **6** 743–757.

Das A, Bose S, Dasgupta S, Roy S and Mukhopadhyay B 2022 Post-Oligocene evolution of Indo-Burma wedge: Insights from deformation structures of Tripura Mizoram fold belt; *J. Struct. Geol.* **154** 104497.

Davis T L 1996 *Geologic map of the Chittagong Hill Tracts, Bangladesh*; Retrieved from http://geologicmapsfoundation.org/images/BangladeshMap12Aug2016.jpg.

Dina N T, Rahman M J J, Hossain M S and Sayem A S M 2016 Provenance of the Neogene succession in the Bandarban structure, South-East Bengal Basin, Bangladesh: Insights from petrography and petrofacies; *J. Himal. Geol.* **37(2)** 141–152.

Duvall A R and Tucker G E 2015 Dynamic ridges and valleys in a strike-slip environment; *J. Geophys. Res. Earth. Sur.* **120** 2016–2026, https://doi.org/10.1002/2015JF003618.

Evans P 1964 The tectonic framework of Assam; *J. Geol. Soc. India* **5** 80–96.

Fryirs K and Brierley G J 2010 Antecedent controls on river character and behaviour in partly confined valley settings: Upper Hunter catchment, NSW, Australia; *Geomorphology* **117** 106–120.

Gani M R and Alam M M 1999 Trench-slope controlled deep-sea clastics in the exposed lower Surma group in the southeastern fold belt of the Bengal Basin, Bangladesh; *Sediment. Geol.* **127(3–4)** 221–236, https://doi.org/10.1016/S0037-0738(99)00050-0.

Gani M R and Alam M M 2004 Fluvial facies architecture in small-scale river systems in the Upper Dupi Tila Formation, northeast Bengal Basin, Bangladesh; *J. Asian Earth Sci.* **24** 225–236, https://doi.org/10.1016/j.jseaes.2003.11.003.

Gahalaut V K, Kundu B, Laishram S S, Catherine J, Kumar A, Singh M D, Tiwari R P, Chadha R K, Samanta S K, Ambikapathy A, Mahesh P, Bansal A and Narsaiah M 2013 Aseismic plate boundary in the Indo-Burmese wedge, northwest Sunda Arc; *Geology* **41(2)** 235–238.

Gilbert O E Jr 2001 Structural geology and regional tectonics of the Chittagong Hills Fold Belt, Eastern Bangladesh; GSA Annual Meeting, Houston, Texas, Abstract 21770.

Govin G, Najman Y, Copley A, Millar I, van der Beek P, Huyghe P, Grujic D and Davenport J 2018 Timing and mechanism of the rise of the Shillong plateau in the Himalayan foreland; *Geology* **46(3)** 279–282.

Haque M M and Roy M K 2021 Geology and sedimentary environment of the Surma Group of rocks, Bandarban anticline, Bandarban, Bangladesh; *J. Nepal Geol. Soc.* **62** 88–106.

Heidbach O, Rajabi M, Reiter K and Ziegler M 2016 World Stress Map, V 1 1 GFZ Data Services.

Hirschmiller J, Grujic D, Bookhagen B, Coutand I, Huyghe P, Mugnier J-L and Ojha T 2014 What controls the growth of the Himalayan foreland fold-and-thrust belt?; *Geology* **42(3)** 247–250, https://doi.org/10.1130/G35057.1.

Holtrop J F and Keizer J 1970 Some aspects of the stratigraphy and correlation of the Surma Basin wells, East Pakistan; *ECAFE Mineral Resources Development Series* **36** 143–154.

Hossain M S, Ao S, Mondal T K, Sain A, Khan M S H, Xiao W and Zhang P 2022 Understanding the deformation structures and tectonics of the active orogenic fold-thrust belt: Insights from the outer Indo-Burman Ranges; *Lithosphere* 6058346.

Hossain M S, Khan M S H, Abdullah R and Mukherjee S 2021 Late Cenozoic transpression at the plate boundary: Kinematics of the eastern segment of the Dauki fault zone (Bangladesh) and tectonic evolution of the petroliferous NE Bengal basin; *Mar. Petrol. Geol.* **131** 105133.

Hossain M S, Khan M S H, Chowdhury K R and Abdullah R 2019 Synthesis of the tectonic and structural elements of the Bengal Basin and its surroundings; In: *Tectonics and Structural Geology: Indian Contex* (ed.) Mukherjee S, Springer International Publishing AG, pp. 135–218, ISBN: 978-3-319-99341-6.

Hossain M S, Xiao W, Khan M S H, Chowdhury K R and Ao S 2020a Geodynamic model and tectono-structural framework of the Bengal Basin and its surroundings; *J. Maps* **16(2)** 445–458.

Hossain, M S, Rahman, M M and Khan R A 2020b Active seismic structures, energy infrastructures, and earthquake disaster response strategy – Bangladesh perspective; *Int. Energy J.* **20(3A)** 509–522, http://www.rericjournal.ait.ac.th/index.php/reric/article/view/2528.

Huang Z, Wang L, Xu M, Zhao D, Mi N and Yu D 2019 *P* and *S* wave tomography beneath the SE Tibetan Plateau: Evidence for lithospheric delamination; *J. Geophys. Res.: Solid Earth* **124** 10,292–10,308.

Huq N E, Haque M M, Rahman M J J and Hamid M L I 2000 Turbidite-like signatures in the exposed sediments of the Bandarban Anticline, south-east Bangladesh; *Bangladesh Geosci. J.* **6** 177–184.

Imam I 2022 Hydrocarbon Resource Potentials of Bangladesh; In: *Bangladesh Geosciences and Resources Potential* (eds) Chowdhury K R, Hossain M S and Khan M S H, 1st edn, CRC Press, Taylor & Francis, USA, pp. 221–258, https://doi.org/10.1201/9781003080817.

Johnson S Y and Alam A M N 1991 Sedimentation and tectonics of the Sylhet trough, Bangladesh; *Geol. Soc. Am. Bull.* **103** 1513–1527, https://doi.org/10.1130/0016-7606(1991)103%3c1513:SATOTS%3e2.3.CO;2.

Kamb W B 1959 Theory of preferred orientation developed by crystallization under stress; *J. Geol.* **67** 153–170.

Khan A A 1991 Tectonics of the Bengal Basin; *J. Himalayan Geol.* **2(1)** 91–101.

Khan M S H, Hossain M S and Uddin M A 2018 Geology and active tectonics of the Lalmai Hills, Bangladesh – an overview from Chittagong Tripura Fold Belt perspective; *J. Geol. Soc. India* **92** 713–720, https://doi.org/10.1007/s12594-018-1093-5.

Khan M S H, Hossain M S and Chowdhury K R 2017 Geomorphic implications and active tectonics of the Sitapahar Anticline – CTFB, Bangladesh; *Bangladesh Geosci. J.* **23** 1–24.

Khin K, Moe A, Aung K P and Zaw T 2023 Structural and tectonic evolution between Indo-Myanmar ranges and central Myanmar basin: Insights from the Kabaw Fault; *Geosys. Geoenviron.* **2(1)** 100176, https://doi.org/10.1016/j.geogeo.2022.100176.

Lisle R J and Leyshon P R 2004 *Stereographic Projection Techniques for Geologists and Civil Engineers* (2nd edn); Cambridge University Press, 112p.

Miall A D 1996 *The Geology of Fluvial Deposits: Sedimentary Facies, Basin Analysis, and Petroleum Geology*; Springer-Verlag, Berlin Heidelberg, 582p.

Miall A D 1978 Lithofacies types and vertical profile models in braided river deposits: A summary; In: *Fluvial Sedimentology* (ed.) Miall A D, Canadian Society of Petroleum Geologists Memoir **5** 597–604.

Mallick R, Lindsey E O, Feng L, Hubbard J, Banerjee P and Hill E M 2019 Active convergence of the India–Burma–Sunda plates revealed by a new continuous GPS network; *J. Geophys. Res.: Solid Earth* **124** 3155–3171.

Maurin T and Rangin C 2009 Structure and kinematics of the Indo-Burmese Wedge: Recent and fast growth of the outer wedge; *Tectonics* **28** TC2010, https://doi.org/10.1029/2008TC002276.

Mandal B C, Woobidullah A S M and Guha D K 2004 Structural style analysis of the Semutang Anticline, Chittagong Hill Tracts, Eastern Fold Belt of the Bengal Basin, Bangladesh; *J. Geol. Soc. India* **64(2)** 211–222.

Mitchell A 1993 Cretaceous-Cenozoic tectonic events in the western Myanmar (Burma)–Assam region; *J. Geol. Soc.* **150(6)** 1089–1102.

Morley C K, Naing T T, Searle M and Robinson S A 2020 Structural and tectonic development of the Indo-Burma ranges; *Earth Sci. Rev.* **200**, https://doi.org/10.1016/j.earscirev.2019.102992.

Najman Y, Bracciali L, Parrish R R, Chisty E and Copley A 2016 Evolving strain partitioning in the Eastern Himalaya: The growth of the Shillong Plateau; *Earth Planet. Sci. Lett.* **433** 1–9, https://doi.org/10.1016/j.epsl.2015.10.017.

Najman Y, Allen R, Willett E A F, Carter A, Barford D, Garzanti E, Wijbrans J, Bickle M, Vezzoli G, Ando S, Oliver G and Uddin M 2012 The record of Himalayan erosion preserved in the sedimentary rocks of the Hatia Trough of the Bengal Basin and the Chittagong Hill Tracts, Bangladesh; *Basin Res.* **24** 499–519, https://doi.org/10.1111/j.1365-2117.2011.00540.x.

Najman Y, Sobel E R, Millar I, Luan X, Zapata S, Garzanti E, Parra M, Vezzoli G, Zhang P, Wa Aung D, Paw S M T L and Lwin T N 2022 The timing of collision between Asia and the West Burma Terrane, and the development of the Indo-Burman Ranges; *Tectonics* **41(7)**, https://doi.org/10.1029/2021TC007057.

Oryan B, Betka P M, Steckler M S, Nooner S L, Lindsey E O, Mondal D, Mathews A M, Akhter S H, Singha S and Than O 2023 New GNSS and geological data from the

Indo-Burman subduction zone indicate active convergence on both a locked megathrust and the Kabaw Fault; *J. Geophys. Res. Solid Earth* **128** e2022JB025550, https://doi.org/10.1029/2022JB025550.

Rahman M J J, Xiao W, Hossain M S, Yeasmin R, Sayem A S M, Ao S, Yang L, Abdullah R and Dina N T 2020 Geochemistry and detrital zircon U–Pb dating of Pliocene-Pleistocene sandstones of the Chittagong Tripura Fold Belt (Bangladesh): Implications for provenance; *Gondwana Res.* **78** 278–290.

Reimann K-U 1993 *Geology of Bangladesh*; Gebrueder Borntraeger, Berlin, 160p.

Replumaz A, Lacassin R, Tapponnier P and Leloup P H 2001 Large river offsets and Plio-Quaternary dextral slip rate on the Red River fault (Yunnan, China); *J. Geophys. Res. Solid Earth* **160(B1)** 819–836.

Rowland S M, Duebendorfer E M and Schiefelbein I M 2007 *Structural Analysis and Synthesis: A Laboratory Course in Structural Geology*; Blackwell publishing, 301p.

Shahriar M U, Hossain D, Hossain M S, Rahman M J J and Kamruzzaman 2020 Geophysical characterization of the Sangu Gas Field, offshore, Bangladesh: Constraints on reservoirs; *J. Petrol. Geol.* **43(4)** 363–382.

Shamsuddin A H M 2022 Petroleum system of Bangladesh and its hydrocarbon reserves and resources; In: *Bangladesh Geosciences and Resources Potential* (eds), Chowdhury K R, Hossain M S and Khan M S H, 1st edn, CRC Press, Taylor & Francis, USA, pp. 157–220, https://doi.org/10.1201/9781003080817.

Sikder A M and Alam M M 2003 2-D modelling of the anticlinal structures and structural development of the eastern fold belt of the Bengal Basin, Bangladesh; *Sediment. Geol.* **155** 209–226, https://doi.org/10.1016/S0037-0738(02)00181-1.

Steckler M S, Mondal D, Akhter S H, Seeber L, Feng L and Gale J 2016 Locked and loading megathrust linked to active subduction beneath the Indo-Burman ranges; *Nat. Geosci.* **9** 615–618, https://doi.org/10.1038/ngeo2760.

Steckler M S, Akhter S H and Seeber L 2008 Collision of the Ganges-Brahmaputra Delta with the Burma Arc; *Earth Planet. Sci. Lett.* **273** 367–378, https://doi.org/10.1016/j.epsl.2008.07.009.

Swanson M T 1988 Pseudotachylyte-bearing strike-slip duplex structures in the Fort Foster brittle zone, S. Maine; *J. Struct. Geol.* **10** 813–828.

Valdiya K S 1996 Antecedent Rivers: Ganges is older than Himalaya; *Resonance* 55–63.

Vorobieva I, Gorshkov A and Mandal P 2021 Modelling the seismic potential of the Indo-Burman megathrust; *Sci. Rep.* **11** 21200, https://doi.org/10.1038/s41598-021-00586-y.

Wang Y, Sieh K, Tun S T, Lai K-Y and Myint T 2014 Active tectonics and earthquake potential of the Myanmar region; *J. Geophys. Res. Solid Earth* **119** 3767–3822.

Westerweel J, Roperch P, Licht A, Dupont-Nivet G, Win Z, Poblete F, Ruffet G, Swe H H, Thi M K and Aung D W 2019 Burma Terrane part of the Trans-Tethyan arc during collision with India according to palaeomagnetic data; *Nat. Geosci.* **12(10)** 863–868.

Woodward N, Boyer S E and Suppe J 1989 Balanced geological cross-sections: An essential technique in geological research and exploration; *Am. Geophys. Union, Washington DC*, https://doi.org/10.1029/SC006.

Yang L, Xiao W, Rahman M J J, Windley B F, Schulmann K, Ao S, Zhang J, Chen Z, Hossain M S and Dong Y 2020 Indo-Burma passive amalgamation along Kaladan Fault: Insights from provenance of Chittagong–Tripura Fold Belt (Bangladesh); *Geol. Soc. Am. Bull.* **132(9–10)** 1953–1968, https://doi.org/10.1130/B35429.1.

Corresponding editor: George Mathew